PDL development will be better understood based on PDL lineage-specific markers, and therapeutic targets for the treatment of periodontal disease may be identified.

Acknowledgements

We would like to thank Drs. Nobuyoshi Shimizu and Takashi Sasaki for assistance with establishing the gene expression profiling database. We are also grateful to Dr. Toshio Teranaka and all the members of the Department of Molecular and Cellular Biochemistry, Osaka University School of Dentistry. This work was supported by a Grant-in-Aid for a High-Tech Research Center Project from the Ministry of Education, Culture, Sports, Science and Technology (MEXT) of Japan, the AGU High-Tech Research Center Project, the 2003 Multidisciplinary Research Project from MEXT, and grants from MEXT.

References

1) MacNeil, R. L., Berry, J. E., Strayhorn, C. L., Shigeyama, Y. and Somerman, M. J. : Expression of type I and XII collagen during development of the periodontal ligament in the mouse. Arch. Oral Biol. **43** : 779—787, 1998.
2) Everts, V., Niehof, A., Jansen, D. and Beertsen, W. : Type VI collagen is associated with microfibrils and oxytalan fibers in the extracellular matrix of periodontium, mesenterium and periosteum. J. Periodontal Res. **33** : 118—125, 1998
3) Lukinmaa, P. L. and Waltimo, J. : Immunohistochemical localization of types I, V, and VI collagen in human permanent teeth and periodontal ligament. J. Dent. Res. **71** : 391—397, 1992.
4) McCulloch, C. A., Lekic, P. and McKee, M. D. : Role of physical forces in regulating the form and function of the periodontal ligament. Periodontology **24** : 56—72, 2000.
5) Bartold, P. and Narayanan, A. : Molecular and cell biology of healthy and diseased periodontal tissues. Periodontology **40** : 29—49, 2006.
6) Somerman, M. J., Ouyang, H. J., Berry, J. E., Saygin, N. E., Strayhorn, C. L. D'Errico, J. A., Hullinger, T. and Giannobile, W. V. : Evolution of periodontal regeneration : from the roots' point of view. J. Periodontal Res. **34** : 420—424, 1999.
7) Melcher, A. H., Cheong, T., Cox, J., Nemeth, E. and Shiga, A. : Synthesis of cementum-like tissue *in vitro* by cells cultured from bone : a light and electron microscope study. J. Periodontal Res. **21** : 592—612, 1986.
8) Bartold, P. M., McCulloch, C. A., Narayanan, A. S. and Pitaru, S. : Tissue engineering : a new paradigm for periodontal regeneration based on molecular and cell biology. Periodontology **24** : 253—269, 2000.
9) Grzesik, W. J. and Narayanan, A. S. : Cementum and periodontal wound healing and regeneration. Crit. Rev. Oral Biol. Med. **13** : 474—484, 2002.
10) Shimono, M., Ishikawa, T., Ishikawa, H., Matsuzaki, H., Hashimoto, S., Muramatsu, T., Shima, K., Matsuzaka, K. and Inoue, T. : Regulatory mechanisms of periodontal regeneration. Microsc. Res. Tech. **60** : 491—502, 2003.
11) Handa, K., Saito, M., Yamauchi, M., Kiyono, T., Sato, S., Teranaka, T. and Narayanan, A. S. : Cementum matrix formation *in vivo* by cultured dental follicle cells. Bone **31** : 606—611, 2002.
12) Seo, B. M., Miura, M., Gronthos, S., Bartold, P. M., Batouli, S., Brahim, J., Young, M., Robey, P. G., Wang, C. Y. and Shi, S. : Investigation of multipotent postnatal stem cells from human periodontal ligament. Lancet **364** : 149—155, 2004.
13) Fujii, S., Maeda, H., Wada, N., Tomokiyo, A., Saito, M. and Akamine, A. : Investigating a clonal human periodontal ligament progenitor/stem cell line *in vitro* and *in vivo*. J. Cell Physiol. **215** : 743—749, 2008.
14) Cho, M. I. and Garant, P. R. : Development and general structure of the periodontium. Periodontology **24** : 9—27, 2000.
15) Sunkin, S. M. and Hohmann, J. G. : Insights from spatially mapped gene expression in the mouse brain. Hum. Mol. Genet. **16** : 209—219, 2007.
16) Chai, Y., Jiang, X., Ito, Y., Bringas, P., Jr., Han, J., Rowitch, D. H., Soriano, P., McMahon, A. P. and Sucov, H. M. : Fate of the mammalian cranial neural crest during tooth and mandibular morphogenesis. Development **127** : 1671—1679, 2000.
17) Saito, M., Iwase, M., Maslan, S., Nozaki, N., Yamauchi, M., Handa, K., Takahashi, O., Sato, S., Kawase, T., Teranaka, T. and Narayanan, A. S. : Expression of cementum-derived attachment protein in bovine tooth germ during cementogenesis. Bone **29** : 242—248, 2001.

18) Bosshardt, D. D. and Schroeder, H. E. : Cementogenesis reviewed : a comparison between human premolars and rodent molars. Anat. Rec. **245** : 267—292, 1996.
19) Ten Cate, A. R. : Development of the periodontium. In : Oral histology, development, structure, and function. (ed. Ten Cate, A. R.), pp.257—275, Mosby. St. Louis, 1994.
20) Yokoi, T., Saito, M., Kiyono, T., Iseki, S., Kosaka, K., Nishida, E., Tsubakimoto, T., Harada, H., Eto, K., Noguchi, T. and Teranaka, T. : Establishment of immortalized dental follicle cells for generating periodontal ligament *in vivo*. Cell Tissue Res. **327** : 301—311, 2007.
21) Morsczeck, C., Gotz, W., Schierholz, J., Zeilhofer, F., Kuhn, U., Mohl, C., Sippel, C. and Hoffmann, K. H. : Isolation of precursor cells (PCs) from human dental follicle of wisdom teeth. Matrix Biol. **24** : 155—165, 2005.
22) Luan, X., Ito, Y., Dangaria, S. and Diekwisch, T. G. : Dental follicle progenitor cell heterogeneity in the developing mouse periodontium. Stem Cells Dev. **15** : 595—608, 2006.
23) Saito, M., Handa, K., Kiyono, T., Hattori, S., Yokoi, T., Tsubakimoto, T., Harada, H., Noguchi, T., Toyoda, M., Sato, S. and Teranaka, T. : Immortalization of cementoblast progenitor cells with Bmi-1 and TERT. J. Bone Miner. Res. **20** : 50—57, 2005.
24) Nishida, E., Sasaki, T., Ishikawa, S. K., Kosaka, K., Aino, M., Noguchi, T., Teranaka, T., Shimizu, N. and Saito, M. : Transcriptome database KK-Periome for periodontal ligament development : expression profiles of the extracellular matrix genes. Gene **404** : 70—79, 2007.
25) Venter, J. C., Levy, S., Stockwell, T., Remington, K., and Halpern, A. : Massive parallelism, randomness and genomic advances. Nat. Genet. **33** Suppl : 219—227, 2003.
26) Lukinmaa, P. L., Vaahtokari, A., Vainio, S., Sandberg, M., Waltimo, J. and Thesleff, I. : Transient expression of type III collagen by odontoblasts : developmental changes in the distribution of pro-alpha 1 (III) and pro-alpha 1 (I) collagen mRNAs in dental tissues. Matrix **13** : 503—515, 1993.
27) Takano-Yamamoto, T., Takemura, T., Kitamura, Y. and Nomura, S. : Site-specific expression of mRNAs for osteonectin, osteocalcin, and osteopontin revealed by *in situ* hybridization in rat periodontal ligament during physiological tooth movement. J. Histochem. Cytochem. **42** : 885—896, 1994.
28) Horiuchi, K., Amizuka, N., Takeshita, S., Takamatsu, H., Katsuura, M., Ozawa, H., Toyama, Y., Bonewald, L. F. and Kudo, A. : Identification and characterization of a novel protein, periostin, with restricted expression to periosteum and periodontal ligament and increased expression by transforming growth factor beta. J. Bone Miner. Res. **14** : 1239—1249, 1999.
29) Yamada, S., Murakami, S., Matoba, R., Ozawa, Y., Yokokoji, T., Nakahira, Y., Ikezawa, K., Takayama, S., Matsubara, K. and Okada, H. : Expression profile of active genes in human periodontal ligament and isolation of PLAP-1, a novel SLRP family gene. Gene **275** : 279—286, 2001.
30) Matheson, S., Larjava, H. and Hakkinen, L. : Distinctive localization and function for lumican, fibromodulin and decorin to regulate collagen fibril organization in periodontal tissues. J. Periodontal Res. **40** : 312—324, 2005.
31) Klar, A., Baldassare, M. and Jessell, T. M. : F-spondin : a gene expressed at high levels in the floor plate encodes a secreted protein that promotes neural cell adhesion and neurite extension. Cell **69** : 95—110, 1992.
32) Tzarfati-Majar, V., Burstyn-Cohen, T. and Klar, A. : F-spondin is a contact-repellent molecule for embryonic motor neurons. Proc. Natl. Acad. Sci. USA **98** : 4722—4727, 2001.
33) Debby-Brafman, A., Burstyn-Cohen, T., Klar, A. and Kalcheim, C. : F-Spondin, expressed in somite regions avoided by neural crest cells, mediates inhibition of distinct somite domains to neural crest migration. Neuron **22** : 475—488, 1999.
34) Ho, A. and Sudhof, T. C. : Binding of F-spondin to amyloid-beta precursor protein : a candidate amyloid-beta precursor protein ligand that modulates amyloid-beta precursor protein cleavage. Proc. Natl. Acad. Sci. USA **101** : 2548—2553, 2004.
35) Kitagawa, M., Kudo, Y., Iizuka, S., Ogawa, I., Abiko, Y., Miyauchi, M. and Takata, T. : Effect of F-spondin on cementoblastic differentiation of human periodontal ligament cells. Biochem. Biophys. Res. Commun. **349** : 1050—1056, 2006.
36) Pispa, J. and Thesleff, I. : Mechanisms of ectodermal organogenesis. Dev. Biol. **262** : 195—205, 2003.
37) Neidhardt, J., Fehr, S., Kutsche, M., Lohler, J. and Schachner, M. : Tenascin-N : characterization of a novel member of the tenascin family that mediates neurite repulsion from hippocampal explants. Mol.

Cell Neurosci. **23** : 193—209, 2003.

38) Kruzynska-Frejtag, A., Wang, J., Maeda, M., Rogers, R., Krug, E., Hoffman, S., Markwald, R. R. and Conway, S. J. : Periostin is expressed within the developing teeth at the sites of epithelial-mesenchymal interaction. Dev. Dyn. **229** : 857—868, 2004.

39) Yamada, S., Tomoeda, M., Ozawa, Y., Yoneda, S., Terashima, Y., Ikezawa, K., Ikegawa, S., Saito, M., Toyosawa, S. and Murakami, S. : PLAP-1/asporin, a novel negative regulator of periodontal ligament mineralization. J. Biol. Chem. **282** : 23070—23080, 2007.

Colloids and Surfaces B: Biointerfaces 66 (2008) 71–76

Contents lists available at ScienceDirect

Colloids and Surfaces B: Biointerfaces

journal homepage: www.elsevier.com/locate/colsurfb

Synthesis of bone formation deriving biosilanes

Norio Yoshino[a,b,*], Kaori Nakajima[a], Keisuke Nakamura[a], Yukishige Kondo[a,b], Katsura Ohashi[c], Tomotaro Nihei[c], Masahiro Saito[d], Toshio Teranaka[c]

[a] Department of Industrial Chemistry, Faculty of Engineering, Tokyo University of Science, 12-1 Ichigaya-Funagawara, Shinjuku, Tokyo 162-0826, Japan
[b] Division of Colloid and Interface Science, Research Institute for Science and Technology, Tokyo University of Science, 1-3 Kagurazaka, Shinjuku, Tokyo 162-8601, Japan
[c] Department of Oral Medicine, Division of Restorative Dentistry, Kanagawa Dental College, 82 Inaoka-cho, Yokosuka, Kanagawa 238-8580, Japan
[d] Department of Biochemistry, Graduate School of Dentistry, Osaka University, 1-8 Yamadaoka, Suita, Osaka 565-0871, Japan

ARTICLE INFO

Article history:
Received 25 February 2008
Accepted 17 May 2008
Available online 24 May 2008

Keywords:
Silane coupling agent having amide group
Biosilane
Bone formation
Cell affinity
Surface modification

ABSTRACT

Six silane coupling agents having amide group (biosilanes) were synthesized with the aim to construct the material surface that allows cells to be compatible with it without their destruction. These agents were expected to make a soft landing to cytoplasm through the hydrogen bonding between their amide groups and cells. Evaluations of cell affinity using glass substrates modified with the synthesized biosilanes revealed that many cells remain on the modified glass plate. In addition, the implantation into the body of immunodeficient mouse of a composite material composed of porous hydroxyapatite and osteoblast showed the formation of a bone-like structure.

1. Introduction

The treatment using mainly autogenous bone graft or artificial material is now performed to cure bone defect parts. There are certain problems involved in the treatment using artificial material, however, such as deterioration in the body of the material and foreign body reaction in which the body recognizes it as a foreign matter. In recent years, much attention has been paid to reproductive medical treatment that allows regeneration of patient's own tissues in the body. Reproductive medical treatment is said to have many advantages including shortened period of treatment, reduction of biomaterial damage, and suppression of foreign body reaction [1–4].

We have synthesized a large number of silane coupling agents and studied the synthesized compounds as surface modifying agent [5–11]. In particular, fluorinated silane coupling agents have been shown to be greatly effective in preventing dental caries and periodontosis, while fluorinated aromatic silane coupling agents have been proved to be unique compounds at present that are usable in thermal nanoimprinting and high-temperature mold releasing as releasing agent heat-resistant up to 350 °C [11].

The present paper describes the synthesis of highly biocompatible and bone formative surface modifying agents for the development of materials used in medical treatment and the examination of cell affinity with the material surface modified with the compounds synthesized. The six surface modifying agents synthesized are amide group-containing silane coupling agents (biosilanes). Note here that amide group, a constituent of proteins, is hydrogen bond formative [12]. After hydroxyapatite (porous), the main component of bone, was treated with a synthesized biosilane, an inorganic/organic composite material with osteoblasts on the biosilane-modified surface was prepared and used in animal experiments. Scheme 1 shows the chemical structures of the biosilanes synthesized in the present work. TI9M was synthesized to study the effect of the silane coupling agent with no N–H bond on cell affinity.

2. Experimental

2.1. Materials

Trimethoxysilane (Tokyo Chemical Ind.) was used after being purified by distillation over calcium hydride (bp 81 °C). Chloroplatinic acid hexahydrate (H_2PtCl_6) (Kojima Chemicals) was used as 0.1 M solution in tetrahydrofuran (THF). THF was used after being

* Corresponding author at: Department of Industrial Chemistry, Faculty of Engineering, Tokyo University of Science, 12-1 Ichigaya-Funagawara, Shinjuku, Tokyo 162-0826, Japan. Tel.: +81 3 5228 8308; fax: +81 3 3235 2214.
E-mail addresses: yoshino@ci.kagu.tus.ac.jp, yoshinonorio2005@yahoo.co.jp (N. Yoshino).

0927-7765/$ – see front matter © 2008 Elsevier B.V. All rights reserved.
doi:10.1016/j.colsurfb.2008.05.009

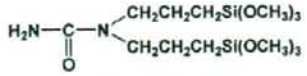

[1,1-DAU6M]

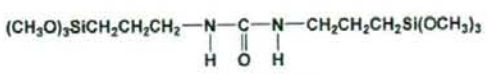

[1,3-DAU6M]

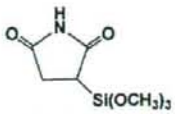

[MI3M]

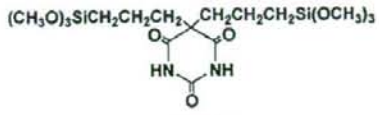

[AB6M]

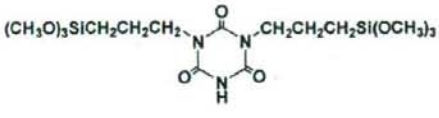

[DI6M]

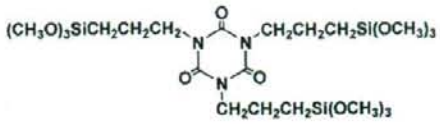

[TI9M]

Scheme 1.

dehydrated over calcium hydride and distilled. 1,1-Diallylurea, 1,3-diallylurea, maleimide, allobarbital, diallylisocyanurate, and triallylcyanurate were used after being dried in a vacuum. The other reagents were used as supplied.

Microcover glass (12 mm × 12 mm × 0.17 mm) (Matsunami Glass Ind.), poly-L-lysine-modified cover glass (Rikaken), and 24-well plate (Falcon) were used as purchased. Phosphate buffer solution (PBS) was prepared by dissolving NaCl (8.0 g), KCl (0.2 g), Na_2HPO_4 (1.15 g), and KH_2PO_4 (0.2 g) in 1000 ml of distilled water and the resultant solution was used after being sterilized in an autoclave. Trypsin/ethylenediamine tetraacetic acid (EDTA) solution was prepared by adding 0.25 vol.% trypsin (GIBCO) to 1 mM aqueous EDTA solution (Wako Pure Chemicals). Culture medium was prepared in a clean bench by adding 10 wt% fetal bovine serum (BioWhittaker), 50 μg/ml ascorbic acid, and each of streptomycin and penicillin at 100 units/ml to minimum essential medium (Sigma). Luciferase assay reagent was prepared by mixing equal volumes of CellTiter-Glo buffer and CellTiter-Glo substrate (both from Promega). KUSA cells (mouse osteoblasts) cultured at 37 °C in a shallow dish were rinsed once with PBS after the supernatant of the culture medium was removed by sucking. After adding 4 ml of trypsin/EDTA solution and exfoliating the cells from the dish, the cells were transferred to a centrifuge tube containing 4 ml of the culture medium. The cells settled by centrifugation (1500 rpm, 5 min) were dispersed in 10 ml of the culture medium and the dispersion was diluted with the medium to give a concentration of 2×10^4 cells/ml. KUSA cell dispersion thus prepared was used to evaluate the cell affinity of the glass surface modified with biosilane.

Hydroxyapatite powder (Hap) (single crystal, Wako) used in FT-IR analysis was used as purchased. Male 5-week-old immunodeficient mice (Nihon Kurea) and β-TCP (75% porosity, pore size 100–400 μm) (Olympus) were used as supplied in transplantation experiment.

2.2. Measurements

FT-IR spectrum was measured by the attenuated total reflection (ATR) method using a Nicolet Avatar 360 FT-IR spectrometer. A Bruker DPX-400 spectrometer was used to measure 400 MHz ^1H NMR spectrum in $CDCl_3$ at room temperature with TMS as internal standard. A JEOL JMS SX102A was used to measure MS by the electron ionization (EI) method. Photoelectron spectroscopic measurement was performed using a JPS-9010C (JEOL) (X-ray source: Mg Kα, pass energy: 30 eV, voltage: 12 kV, current: 5 mA).

A chemiluminescence analyzer Fuji LAS 3000 (Fuji Film), an optical microscope Olympus CKX41 (Olympus), a centrifuge Kubota 6200 (Kubota), an incubator (37 °C, CO_2 5%) (Thermo Steri-Cycle CO_2 incubator), a clean bench Sanyo Class2 typeA/B3 (Sanyo), and a rotary microtome IVS-400 (Sakura Finetek, Japan) were used in cell affinity evaluating test and animal experiment.

2.3. Synthesis of biosilane

Scheme 2 shows the synthetic route.

2.3.1. Synthesis of 1,1-DAU6M

1,1-Diallylurea (3.98 g, 28.4 mmol), THF (10 ml), and 0.1 M chloroplatinic acid hexahydrate solution in THF (0.1 ml) were taken into a 100 ml round bottom flask equipped with a dropping funnel and a reflux condenser and trimethoxysilane (7.22 ml, 56.8 mmol) was added slowly in 30 min in a nitrogen atmosphere to the reaction mixture while heating at its boiling point (ca. 76 °C). The mixture was further heated for 20 h at the boiling point of the mixture. The product was obtained as a colorless transparent liquid after the solvent was removed at a reduced pressure and the residue was distilled in a vacuum (bp 110 °C/40 Pa). The yield was 65% (7.09 g). The spectral data are given in Section 3.1.1.

2.3.2. Synthesis of 1,3-DAU6M

1,3-Diallylurea (1.34 g, 9.57 mmol), THF (10 ml), and 0.1 M chloroplatinic acid hexahydrate solution in THF (0.1 ml), and trimethoxysilane (2.43 ml, 19.1 mmol) were used to synthesize the compound in the same way as in Section 2.3.1. The product was obtained as a colorless transparent liquid (bp 88 °C/10 Pa) in a yield of 82% (3.01 g). The spectral data are given in Section 3.1.2.

2.3.3. Synthesis of MI3M

MI3M was synthesized using maleimide (3.32 g, 34.2 mmol), THF (10 ml), 0.1 m chloroplatinic acid hexahydrate solution in THF

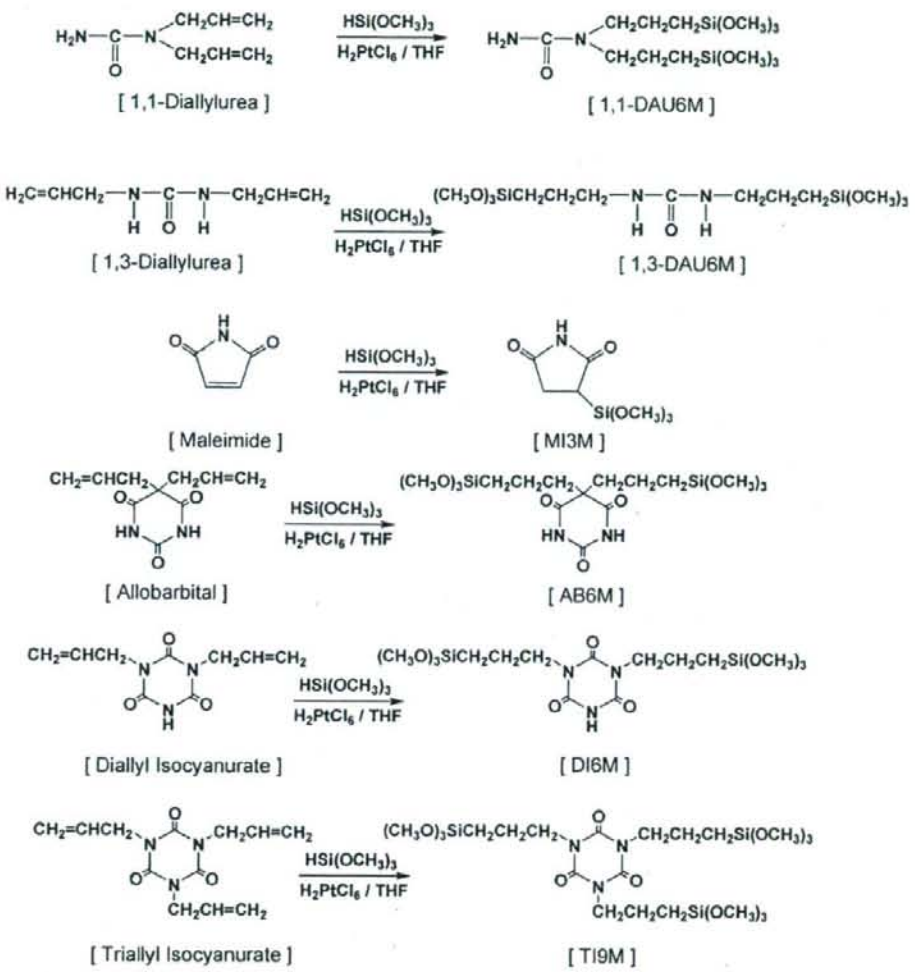

Scheme 2.

(0.1 ml), and trimethoxysilane (4.35 ml, 34.2 mmol) in a similar way to that in Section 2.3.1. The product was obtained as a white solid (bp 105 °C/10 Pa) in a yield of 56% (4.20 g). The spectral data are given in Section 3.1.3.

2.3.4. Synthesis of AB6M

AB6M was synthesized using allobarbital (5.00 g, 24.0 mmol), THF (10 ml), 0.1 M chloroplatinic acid hexahydrate solution in THF (0.1 ml), and trimethoxysilane (6.11 ml, 48.1 mmol) as in Section 2.3.1. The product was obtained as a white solid (bp 250 °C/200 Pa) in a yield of 83% (9.02 g). The spectral data are given in Section 3.1.4.

2.3.5. Synthesis of DI6M

DI6M was synthesized using diallyl isocyanurate (3.00 g, 14.3 mmol), THF (10 ml), 0.1 M chloroplatinic acid hexahydrate solution in THF (0.1 ml), and trimethoxysilane (3.65 ml, 28.7 mmol) as in Section 2.3.1. The product was obtained as a white solid (bp 220 °C/60 Pa) in a yield of 86% (5.59 g). The spectral data are given in Section 3.1.5.

2.3.6. Synthesis of TI9M

TI9M was synthesized using triallylisocyanurate (4.28 g, 17.2 mmol), THF (10 ml), 0.1 M chloroplatinic acid hexahydrate solution in THF (0.1 ml), and trimethoxysilane (6.55 ml, 60.1 mmol) as in Section 2.3.1. The product was obtained as a colorless transparent liquid (bp 205 °C/40 Pa) in a yield of 80% (8.46 g). The spectral data are given in Section 3.1.6.

2.4. In vitro study

2.4.1. Surface modification of cover glass plates

Microcover glass plates were used after being immersed in 1 M aqueous sodium hydroxide for 1 h and in 1 M nitric acid for 1 h, rinsed thoroughly with ion exchanged water, and dried in a vacuum [13]. The cover glasses were then immersed in 10 mM ethanolic

solution of each of the biosilanes for 24 h at room temperature, washed with ethanol, and dried to give biosilane-modified cover glass plates (abbreviated hereafter to modified glass substrates). Modified glass substrates were surface-analyzed using XPS.

2.4.2. Cell viability assay

Modified glass substrates were prepared as in Section 2.4.1 and poly-L-lysine modified cover glass plates as positive control were set in 24-well plates, washed once with ethanol and five times with PBS, and dried. The cell dispersion (400 μl) was placed in each of the 24-well plates and the cells were incubated for 1 h at 37 °C in an incubator. The 24-well plates were then washed twice with PBS and the cells in each plate were observed under the optical microscope. The results are given in Section 3.2.2. PBS (200 μl) and the luciferase assay reagent (200 μl) were prepared as in Section 2.1 and added to each of the well plates and the luminescence from each well plate was detected with the chemiluminescence detecting apparatus after the plates were allowed to stand for 10 min in the dark. The results are given in Section 3.2.3.

2.5. In vivo study

2.5.1. Surface modification of hydroxyapatite and β-TCP

The following experiments were performed to analyze the modified surface by FT-IR. HAp powder (single crystal, 1 g) was placed in 1 mM ethanolic 1,1-DAU6M solution and the mixture was stirred for 24 h at room temperature. The powder was washed five times with 10 ml of ethanol for each washing and dried in a vacuum. The modified HAp powder was surface-analyzed by FT-IR using the KBr tablet method. The results are given in Section 3.3.1.

β-TPC was immersed in 50 mM ethanolic 1,1-DAU6M solution for 24 h at room temperature. The modified β-TPC was dried in the air and sterilized in an ethylene oxide gas atmosphere at 50 °C. β-TPC/osteoblast composite was obtained by incubating the modified β-TPC in the culture medium containing 1×10^6 osteoblasts for 12 h at 37 °C.

2.5.2. Implantation experiment of β-TPC/osteoblast composite using immunodeficient mouse

β-TPC/osteoblast composite together with unmodified β-TPC as control were subcutaneously implanted into the back skin of an immunodeficient mouse and they were taken out 8 weeks later. The implanted samples taken out of the animal were immersed in 4% paraformaldehyde solution at 4 °C for 12 h to fix them (stoppage of tissue denaturation). The fixed samples were washed for 10 min in a running water and the water in the sample tissues was replaced by ethanol and then toluene after being decalcificated in 10% aqueous formic acid solution for 2 days. The samples thus oleophilized were immersed in melted paraffin to allow the liquid to penetrate into them. Then, the samples embedded in paraffin were sliced into 3 μm thick layers with a rotary microtome for histological observation and each layer was dyed with hematoxyline–eosine to be observed under the optical microscope. Positively charged hematoxyline is bound to negatively charged phosphate group of cell nucleus and develops an indigo-blue color while negatively charged eosine is attached to positively charged cytoplasm developing a red or dark red color.

3. Results and discussion

3.1. Synthesis of biosilanes

3.1.1. Synthesis of 1,1-DAUM6M

IR (cm^{-1}) 3346 (ν_{N-H}), 2841–2939 (ν_{C-H}), 1648 ($\nu_{C=O}$), 1057 (ν_{Si-O}); ^1H NMR ($CDCl_3$) δ0.61–0.66 (CH_2Si, t (triplet), 4H; J = 20 Hz), 1.57–1.65 ($CH_2CH_2CH_2$, m (multiplet), 4H), 3.15–3.19 (N–CH_2, t, 4H; J = 16 Hz), 3.53–3.57 (CH_3, s (singlet), 18H), 4.63–4.69 (NH_2, s, 2H); MS (*m*/*z*) (relative intensity with max peak), 384 (4.0) $[M]^+$, 340(22)$[M\text{-}CONH_2]^+$, 160(100)$[CH_2CH_2CH_2Si(OCH_3)_3]^+$, 121 (52) $[Si(OCH_3)_3]^+$, 91 (45) $[Si(OCH_3)_2]^+$.

3.1.2. Synthesis of 1,3-DAUM6M

IR (cm^{-1}) 3334 (ν_{N-H}), 2837–2935 (ν_{C-H}), 1628 ($\nu_{C=O}$), 1073 (ν_{Si-O}); ^1H NMR ($CDCl_3$) δ0.63–0.67 (CH_2Si, t, 4H; J = 16 Hz), 1.59–1.63 ($CH_2CH_2CH_2$, m, 4H), 3.13–3.16 (NH–CH_2, t, 4H; J = 12 Hz), 3.54–3.57 (CH_3, s, 18H), 4.34–4.49 (NH, s, 2H); MS (*m*/*z*) (rel int), 384 (12) $[M]^+$, 121 (86) $[Si(OCH_3)_3]^+$, 91 (34) $[Si(OCH_3)_2]^+$.

3.1.3. Synthesis of MI3M

IR (cm^{-1}) 3278 (ν_{N-H}), 2842–2947 (ν_{C-H}), 1716 ($\nu_{C=O}$), 1090 (ν_{Si-O}); ^1H NMR ($CDCl_3$) δ2.75–2.77 (CHSi, s, 1H), 2.78–2.82 (CH_2, d (doublet), 2H; J = 16 Hz), 3.60–3.76 (CH_3, s, 9H), 7.86–8.37 (NH, s, 1H); MS (*m*/*z*) (rel int), 219 (100) $[M]^+$, 121 (42) $[Si(OCH_3)_3]^+$, 91 (24) $[Si(OCH_3)_2]^+$.

3.1.4. Synthesis of AB6M

IR (cm^{-1}) 3215 (ν_{N-H}), 2842–2951 (ν_{C-H}), 1711 ($\nu_{C=O}$), 1085 (ν_{Si-O}); ^1H NMR ($CDCl_3$) δ0.56–0.60 (CH_2Si, t, 4H; J = 16 Hz), 1.28–1.32 ($CH_2CH_2CH_2$, m, 4H), 1.98–2.02 (C–CH_2, t, 4H; J = 16 Hz), 3.53–3.57 (CH_3, s, 18H), 8.11 (NH, s, 2H); MS (*m*/*z*) (rel int), 451 (3.0) $[M]^+$, 121 (65) $[Si(OCH_3)_3]^+$, 91 (20) $[Si(OCH_3)_2]^+$.

3.1.5. Synthesis of DI6M

IR (cm^{-1}) 3248 (ν_{N-H}), 2847–2946 (ν_{C-H}), 1673 ($\nu_{C=O}$), 1085 (ν_{Si-O}); ^1H NMR ($CDCl_3$) δ0.63–0.67 (CH_2Si, t, 4H; J = 16 Hz), 1.72–1.77 ($CH_2CH_2CH_2$, m, 4H), 3.56–3.60 (CH_3, s, 18H), 3.82–3.85 (N–CH_2, t, 4H; J = 12 Hz), 7.95 (NH, s, 1H); MS (*m*/*z*) (rel int), 453 (4.0) $[M]^+$, 121 (100) $[Si(OCH_3)_3]^+$, 91 (26) $[Si(OCH_3)_2]^+$.

3.1.6. Synthesis of TI9M

IR (cm^{-1}) 2847–2946 (ν_{C-H}), 1689 ($\nu_{C=O}$), 1085 (ν_{Si-O}); ^1H NMR ($CDCl_3$) δ0.63–0.67 (CH_2Si, t, 6H; J = 16 Hz), 1.71–1.75 ($CH_2CH_2CH_2$, m, 6H), 3.56–3.59 (CH_3, s, 27H), 3.82–3.86 (N–CH_2, t, 6H; J = 16 Hz);

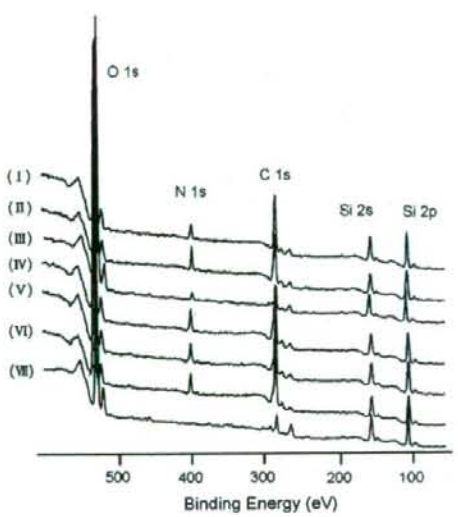

Fig. 1. XPS spectra of glass surfaces modified with 1,1-DAU6M (I), 1,3-DAU6M (II), MI3M (III), AB6M (IV), DI6M (V), and TI9M (VI), and unmodified one (VII).

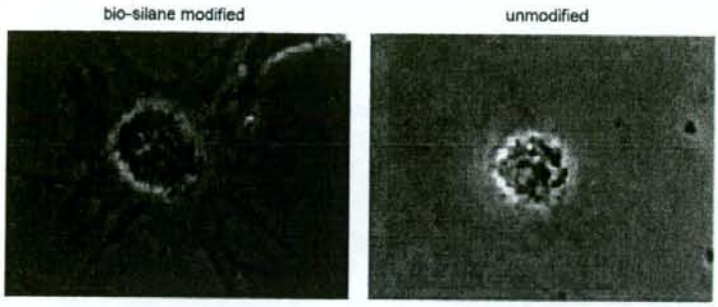

Fig. 2. Photomicrographs of cell adsorption onto biosilane-modified and -unmodified glass surfaces.

MS (*m*/*z*) (rel int), 615 (4.0) $[M]^+$, 121 (100) $[Si(OCH_3)_3]^+$, 91 (18) $[Si(OCH_3)_2]^+$.

3.2. In vitro study

3.2.1. Surface analysis of cover glass

Fig. 1 shows the XPS spectra of glass substrates modified with 1,1-DAU6M, 1,3-DAU6M, MI3M, AB6M, DI6M, and TI9M, together with the spectrum of unmodified glass substrate [14,15]. All substrates exhibited peaks due to Si (2p), Si (2s), C (1s), and O (1s) at around 100, 150, 285, and 530 eV, respectively. In addition, a peak due to N (1s) was observed at around 400 eV for the modified substrates though this peak was not observed for the unmodified substrate, suggesting strongly that the glass substrate was modified with biosilane.

3.2.2. Microscopy

Fig. 2 shows typical optical microscopic images of KUSA cells on the biosilane-modified and unmodified glass substrates. Spherical cells were observed on the modified glass substrate indicating the physically adsorbed cells while somewhat spread cells were observed on the unmodified glass substrate, which shows a high affinity of the cells to the substrate [16].

3.2.3. Relative luminescence intensity

Fig. 3 shows the results of luciferase assay. The luminescence is caused by adenosine triphosphate (ATP) in the cells and its intensity is proportional to cell number [17,18]. Luminescence intensity for the biosilane-modified glass substrates was higher than that for the unmodified substrate, especially the substrates modified with 1,1-DAU6M, 1,3-DAU6M, and AB6M showed an intensity as high as or higher than that for poly-L-lysine-modified glass substrate (poly-L-lysine is a commercially available polymer that exhibits a high affinity to biological cells and used in this work as control). In fact, about 20 times cells were observed on the poly-L-lysine-modified glass substrate when compared with the number of cells on the unmodified substrate. In addition, the intensity of luminescence tended to increase with increasing number of amide groups in biosilane molecule.

3.3. In vivo study

3.3.1. FT-IR spectra of hydroxyapatite modified with 1,1-DAU6M

Fig. 4 shows the FT-IR spectra of 1,1-DAU6M (A), HAp modified with 1,1-DAU6M (B), and unmodified HAp (C). A peak was observed at around 2800 cm^{-1} due to C–H stretching vibration of 1,1-DAU6M in (B). No peak was observed at this wave number in (C), suggesting that HAp was modified with 1,1-DAU6M.

3.3.2. HE stained images

Fig. 5 shows the image of an implanted piece stained with hematoxyline–eosin obtained in the implantation experiment

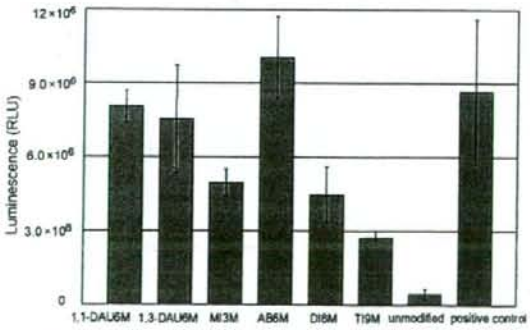

Fig. 3. Relative luminescence intensities of cells adsorbed onto glass surfaces after incubation at 37 °C for 1 h.

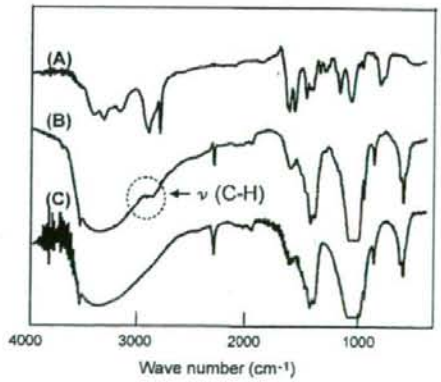

Fig. 4. FT-IR spectra of (A) 1,1-DAU6M monomer, (B) 1,1-DAU6M-modified HAp particle, and (C) unmodified HAp particle.

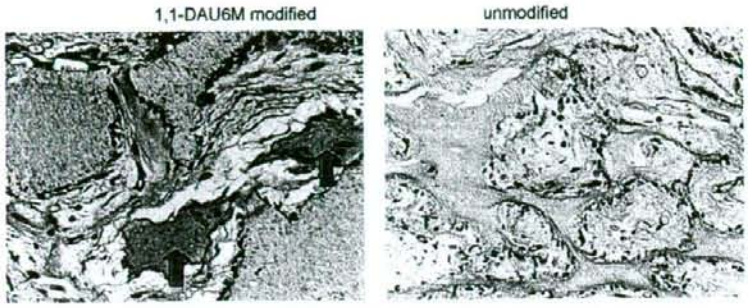

Fig. 5. Hematoxyline–eosin stained images of 1,1-DAU6M modified (two arrows) and unmodified β-TCP/cell composite materials.

using mouse and β-TCP/osteoblast composite. While a bone-like structure was observed in the interior of this composite, no such structure was found for unmodified β-TCP. This would be interpreted as indicating that osteoblasts are hardly fixed on unmodified β-TCP, whereas the cells easily attach to the modified β-TCP through the interaction of amide groups of biosilane on its surface with the cells, thereby making the cells possible to wander into the interior of β-TCP.

4. Conclusions

Six amide group-possessing biosilane were synthesized with the aim to construct the material surface that allows biological cells to be compatible with it. These agents were expected to make a soft landing on cytoplasm without cell destruction through the hydrogen bonding between their amide groups and biological cells. Glass substrates modified with the synthesized biosilanes exhibited a high affinity to biological cells *in vitro*. Very few biological cells were found on the surface of glass substrate modified with silane coupling agent having no amide group. A bone-like structure was observed in the interior of a composite material prepared from β-TCP modified with one of the biosilanes synthesized in this work, 1,1-DAU6M, and osteoblasts in an implantation experiment into an immunodeficient mouse. The biosilanes prepared in this work are expected to greatly contribute to the future bone-regenerating medical treatment.

Acknowledgement

This work was supported in part by Grants-in-Aid for Scientific Research (B) (No. 19390487) from the Ministry of Education, Science, Sports, and Culture of Japan.

References

[1] R. Langer, J.P. Vacanti, Science 260 (1993) 920.
[2] J. Goshima, V.M. Goldberg, A.I. Caplan, Biomaterials 12 (1991) 253.
[3] J.A. Thomson, J. Itskovitz-Eldor, S.S. Shapiro, M.A. Waknitz, J.J. Swiergiel, V.S. Marshall, J.M. Jones, Science 282 (1998) 1145.
[4] J. Song, V. Malaythong, C.R. Bertozzi, J. Am. Chem. Soc. 127 (2005) 3366.
[5] N. Yoshino, Y. Yamamoto, T. Seto, S. Tominaga, T. Kawase, Bull. Chem. Soc. Jpn. 66 (1993) 472.
[6] N. Yoshino, Y. Yamamoto, K. Hamano, T. Kawase, Bull. Chem. Soc. Jpn. 66 (1993) 1754.
[7] N. Yoshino, H. Nakaseko, Y. Yamamoto, React. Polym. 23 (1994) 157.
[8] N. Yoshino, A. Sasaki, T. Seto, J. Fluorine Chem. 71 (1995) 21.
[9] N. Yoshino, Y. Kondo, T. Yamaguchi, J. Fluorine Chem. 79 (1996) 87.
[10] N. Yoshino, T. Teranaka, J. Biomater. Sci., Polym. Ed. 8 (1997) 623.
[11] N. Yoshino, T. Sato, K. Miyao, M. Furukawa, Y. Kondo, J. Fluorine Chem. 127 (2006) 1058.
[12] G.E. Douberly, S. Pan, D. Walters, H. Matsui, J. Phys. Chem. B 105 (2001) 7612.
[13] P. Filippini, G. Rainaldi, A. Ferrante, B. Mecheri, G. Gabrielli, M. Bombace, P.L. Indovina, M.T. Santini, J. Biomed. Mater. Res. 55 (2001) 338.
[14] T.K. Kim, X.M. Yang, R.D. Peters, B.H. Sohn, P.F. Nealey, J. Phys. Chem. B 104 (2000) 7403.
[15] N. Adden, L.J. Gamble, D.G. Castner, A. Hoffmann, G. Gross, H. Menzel, Langmuir 22 (2006) 8197.
[16] C.S. Chen, M. Mrksich, S. Huang, G.M. Whitesides, D.E. Ingber, Science 276 (1997) 1425.
[17] R.L. Klemke, M. Yebra, E.M. Bayna, D.A. Cheresh, Cell Biol. 127 (1994) 859.
[18] A.L. Prieto, G.M. Edelman, K.L. Crossin, Cell Biol. 90 (1993) 10154.

THE JOURNAL OF BIOLOGICAL CHEMISTRY VOL. 283, NO. 6, pp. 3385–3391, February 8, 2008
Printed in the U.S.A.

Neurotrophic Factor Neurotrophin-4 Regulates Ameloblastin Expression via Full-length *TrkB*[*][S]

Received for publication, June 14, 2007, and in revised form, October 31, 2007 Published, JBC Papers in Press, November 28, 2007, DOI 10.1074/jbc.M704913200

Keigo Yoshizaki[‡§], Shinya Yamamoto[‡], Aya Yamada[‡], Kenji Yuasa[‡], Tsutomu Iwamoto[‡], Emiko Fukumoto[¶], Hidemitsu Harada[‖], Masahiro Saito[**], Akihiko Nakasima[§], Kazuaki Nonaka[‡], Yoshihiko Yamada[‡‡], and Satoshi Fukumoto[‡§§1]

From the Section of [‡]Pediatric Dentistry and [§]Orthodontics, Division of Oral Health, Growth, and Development, Faculty of Dental Science, Kyushu University, Fukuoka 812-8582, Japan, [¶]Nagasaki University Graduate School of Biomedical Sciences, Nagasaki 852-8521, Japan, the [‖]Department of Oral Anatomy II, Iwate Medical College School of Dentistry, Morioka, Iwate 020-8505, Japan, the [**]Department of Molecular and Cellular Biochemistry, Osaka University Graduate School of Dentistry, Suita, Osaka 565-0871, Japan, the [‡‡]Craniofacial Developmental Biology and Regeneration Branch, NIDCR, National Institutes of Health, Bethesda, Maryland 20892, and the [§§]Division of Pediatric Dentistry, Department of Oral Health and Development Sciences, Tohoku University Graduate School of Dentistry, Sendai, Miyagi 980-8575, Japan

Neurotrophic factors play an important role in the development and maintenance of not only neural but also nonneural tissues. Several neurotrophic factors are expressed in dental tissues, but their role in tooth development is not clear. Here, we report that neurotrophic factor neurotrophin (NT)-4 promotes differentiation of dental epithelial cells and enhances the expression of enamel matrix genes. Dental epithelial cells from 3-day-old mice expressed NT-4 and three variants of *TrkB* receptors for neurotrophins (full-length *TrkB-FL* and truncated *TrkB-T1* and *-T2*). Dental epithelial cell line HAT-7 expressed these genes, similar to those in dental epithelial cells. We found that NT-4 reduced HAT-7 cell proliferation and induced the expression of enamel matrix genes, such as ameloblastin (Ambn). Transfection of HAT-7 cells with the *TrkB-FL* expression construct enhanced the NT-4-mediated induction of Ambn expression. This enhancement was blocked by K252a, an inhibitor for *Trk* tyrosine kinases. Phosphorylation of ERK1/2, a downstream molecule of *TrkB*, was induced in HAT-7 cells upon NT-4 treatment. *TrkB-FL* but not *TrkB-T1* transfection increased the phosphorylation level of ERK1/2 in NT-4-treated HAT-7 cells. These results suggest that NT-4 induced Ambn expression via the *TrkB*-MAPK pathway. The p75 inhibitor TAT-pep5 decreased NT-4-mediated induction of the expression of Ambn, *TrkB-FL*, and *TrkB-T1*, suggesting that both high affinity and low affinity neurotrophin receptors were required for NT-4 activity. We found that NT-4-null mice developed a thin enamel layer and had a decrease in Ambn expression. Our results suggest that NT-4 regulates proliferation and differentiation of the dental epithelium and promotes production of the enamel matrix.

Mammalian development is a complex and highly orchestrated process that involves intricate cross-talk between growth factors and other regulatory molecules. The interaction between the epithelium and mesenchyme induces specific molecular and cellular changes that lead to organogenesis. These interactions are particularly crucial during the initiation of the development of ectodermal organs, such as teeth, skin, hair, and mammary and prostate glands (1). The oral epithelium provides the initial signaling for neuronal crest-derived ectomesenchyme development, and then both tissues interact during tooth formation. Various transcription factors, growth factors, and extracellular matrices are expressed by enamel matrix-producing ameloblasts during tooth development (2–4). The principal components of the enamel matrix that are synthesized by secretory ameloblasts can be classified into two major categories, amelogenin (Amel)[2] and non-Amel, which includes ameloblastin (Ambn) and enamelin (Enam) (5). Ambn, also known as amelin or sheathlin, is a tooth-specific glycoprotein that represents the most abundant non-Amel enamel matrix protein. We previously created Ambn-null mice, which develop severe enamel hypoplasia in which ameloblasts detached from the matrix, lost cell polarity, resumed proliferation, and formed multiple cell layers (6). These results suggest that Ambn is essential for ameloblast differentiation and enamel formation.

Nerve growth factor (NGF), brain-derived neurotrophic factor (BDNF), and neurotrophin-3 and -4/5 (NT-3 and NT-4/5, respectively) are structurally and functionally related and belong to the neurotrophin family, which promotes the development and survival of the vertebrate nervous system (7). Neurotrophins interact with two classes of cell surface receptors. The first class is *Trk* tyrosine kinase receptors that bind neurotrophins with a high affinity (8). *TrkA* mediates the biological

* This work was supported in part by Grants-in-aid for Research Fellows 15689025, 17689058, 19791585, and 17659650 from the Japan Society for the Promotion of Science and the Ministry of Education, Science, and Culture of Japan (to S. F., A. Y., and K. N.). The costs of publication of this article were defrayed in part by the payment of page charges. This article must therefore be hereby marked "*advertisement*" in accordance with 18 U.S.C. Section 1734 solely to indicate this fact.

[S] The on-line version of this article (available at http://www.jbc.org) contains supplemental Table 1 and Figs. 1–3.

[1] To whom correspondence should be addressed: Division of Pediatric Dentistry, Dept. of Oral Health and Development Sciences, Tohoku University Graduate School of Dentistry, Sendai, Miyagi 980-8575, Japan. Fax: 81-22-717-8380; E-mail: fukumoto@mail.tains.tohoku.ac.jp.

[2] The abbreviations used are: Amel, amelogenin; BrdUrd, bromo-2′-deoxyuridine; MAPK, mitogen-activated protein kinase; ERK, extracellular signal-regulated kinase; Ambn, ameloblastin; Enam, enamelin; NGF, neural growth factor; BDNF, brain-derived neurotrophic factor; NT, neurotrophin; PBS, phosphate-buffered saline; RT, reverse transcriptase; MEK, mitogen-activated protein kinase/extracellular signal-regulated kinase kinase; P1, P3, and P7, postnatal day 1, 3, and 7, respectively.

response of NGF, *TrkC* is activated by NT-3, and BDNF and NT-4/5 are the preferred ligands for *TrkB* (7). *TrkB* and *TrkC* have truncated transcripts at the C terminus (9–12). The second class is the common low affinity neurotrophin receptor, p75, which does not have a tyrosine kinase domain (13, 14). Further, neurotrophins have other regulatory roles during embryogenesis. NGF is a mitogenic factor for human epithelial cells (15), and NT-3 stimulates the proliferation of migratory neural crest cells (16). The expression of p75 may be required for kidney morphogenesis (17) and also promote apoptosis (18, 19). In the skin, the expression of BDNF and NT-4 is strikingly dependent on the hair cycle and peaks during spontaneous, apoptosis-driven hair follicle regression, known as catagen. NT-4 was also reported to accelerate catagen development in murine skin organ cultures. These results suggest that NT-4 is useful as an agent of hair growth control.

During tooth development, neurotrophic factors and their receptors are expressed in the tooth germ (20). However, their role in tooth development has not been elucidated. At the initiation stages of tooth germ development, NGF is expressed in the dental mesenchyme and weakly in the dental epithelium. At the bud stage, the majority of dental epithelial cells have lost their NGF expression, although NGF is still expressed in the inner dental epithelium and condensed mesenchyme. During later embryonic and early postnatal tooth development, NGF can be observed in the dental follicles. At the bell stage, NGF appears in epithelial cells of the stratum intermedium, whereas after birth it is restricted to cells located in the cervical part of the enamel organ. In the postnatal period, NGF is also detected in the dental papilla mesenchyme. BDNF is expressed in the region of developing rat teeth as well as in the mesenchyme under the developing skin of the mandibular process (20). In postnatal animals, BDNF is mainly detected in the dental papilla, and its expression pattern is correlated with the onset of dental innervation (21). NT-3 is expressed throughout the mesenchyme of the mandibular process at the initiation stage, whereas it appears in the epithelial cervical loops in the cap stage. During later stages, NT-3 expression is gradually restricted to the more cervical parts of the inner enamel epithelium and is no longer detected in postnatal tooth germs (20). The expression of NT-4 is restricted to epithelial cells. During subsequent development, expression persists in all dental epithelium components, including ameloblasts and the outer enamel epithelium as well as in the dental lamina (20, 21). Among neurotrophic factors, NT-4 is the only one detected in differentiated ameloblasts. These findings suggest that NT-4 may be important for dental epithelium differentiation and maintenance of ameloblast functions. However, the role of NT-4 in tooth development is unknown.

In the present study, we investigated the roles of NT-4 and *TrkB* in tooth development *in vitro* using dental epithelium cultures and *in vivo* using NT-4 knock-out mice. NT-4 and *TrkB* receptors were expressed in the dental epithelium of 3-day-old mice and in the HAT-7 dental epithelial cell line. We found that NT-4 inhibited proliferation and induced differentiation of HAT-7 cells. NT-4 treatment of HAT-7 cells increased mRNA expression for enamel matrix proteins Ambn, Enam, and dentin sialophosphoprotein. Further, NT-4-mediated induction of Ambn expression was regulated by the full-length *TrkB-FL* receptor and ERK1/2 pathway. In NT-4 knock-out mice, Ambn expression was dramatically reduced, and the enamel layer was thin. Our findings suggest that NT-4 plays a role in proliferation and differentiation of the dental epithelium and is required for the expression of enamel matrix genes.

EXPERIMENTAL PROCEDURES

Cell Culture and Transfection—HAT-7 cells, an epithelial cell line, and mDP cells, a dental mesenchymal cell line, were maintained in Dulbecco's modified Eagle's medium/F-12 medium supplemented with 10% fetal bovine serum and 1% penicillin and streptomycin at 37 °C in a humidified atmosphere containing 5% CO_2 (22). To transfect with the expression vectors for *TrkB*, HAT-7 cells were plated in a 60-mm plastic tissue culture plate (Falcon) at a density of 1×10^6 cells/3 ml/plate. To facilitate the detection of protein expression, V5 and His tags were fused to the C terminus of the two rat *TrkB* isoforms, *TrkB-FL* and *TrkB-T1*. *TrkB-FL* and *TrkB-T1* cDNA were prepared from adult rat brain mRNA by RT-PCR and confirmed by DNA sequencing. The forward primer for *TrkB-FL* and *TrkB-T1* was 5′-CTCTGACTGACTGGCACTGG-3′, and the reverse primer was 5′-GCCTAGGATGTCCAGGTAGACGGGC-3′ for *TrkB-FL* or 5′-CCCATCCAGGGGGATCTTA-3′ for *TrkB-T1*. PCR was performed at 94 °C for 30 s, 60 °C for 30 s, and 72 °C for 60 s for 30 cycles. The PCR products were cloned into pEF6/V5-His-TOPO® (Invitrogen) according to the manufacturer's protocol. Cells were transfected using Lipofectamine 2000 (Invitrogen) according to the manufacturer's protocol. Stable transfectant cells for *TrkB-FL* and *TrkB-T1* were selected in the presence of 5 μg/ml Blasticidin (Invitrogen).

Cell Proliferation and Bromodeoxyuridine (BrdUrd) Incorporation—Cells were plated at 1×10^5 cells/ml/well in 12-well plates for 24 h. Cell numbers were determined using a trypan blue dye exclusion method. For the BrdUrd incorporation assay, cells were incubated at the same cell density described above for 24 h prior to the addition of various growth factors. After treatments with various growth factors, BrdUrd (Sigma) was added to the plates (10 μM) for 30 min, and then the cells were fixed with cold methanol for 10 min, rehydrated in phosphate-buffered saline (PBS), and incubated for 30 min in 1.5 M HCl. After washing three times in PBS, the plates were incubated with a 1:50 dilution of fluorescein isothiocyanate-conjugated anti-BrdUrd antibody (Roche Applied Science) for 30 min at room temperature. Finally, the cells were washed in PBS three times and incubated with 10 μg/ml propidium iodide (Sigma) in PBS for 30 min at room temperature. BrdUrd-positive cells were examined under a microscope (Biozero-8000; Keyence, Japan).

Western Blotting—Cells were plated in 12-well plates at 1×10^5 cells/well for 1 day prior to NT-4 treatment. The cells were then treated with 100 ng/ml NT-4 for 0–60 min at 37 °C. Thereafter, they were washed twice with ice-cold 1 mM sodium orthovanadate (Sigma) in PBS, lysed with Nonidet P-40 buffer supplemented with a proteinase inhibitor mixture (Sigma) and phenylmethanesulfonyl fluoride at 4 °C for 10 min, and centrifuged, and then the supernatants were transferred to a fresh

tube. The cell lysates were separated by 12% SDS-PAGE and analyzed by Western blotting. The blotted membrane was incubated with antibodies, and the signals were detected with an ECL kit (Amersham Biosciences). ERK and second antibodies were purchased from Cell Signaling.

RNA Isolation and RT-PCR—Developing molars were dissected from mice on postnatal day 1 (P1), P3, and P7. Epithelial and mesenchymal tissues were separated from tooth germ from P3 mice under a microscope. Total RNA was isolated using TRIzol (Invitrogen) according to the manufacturer's protocol. First strand cDNA was synthesized at 42 °C for 90 min using oligo$(dT)_{14}$ primer with SuperScript III (Invitrogen). PCR amplification was performed using the primers listed in supplemental Table 1. The PCR products were separated on a 1.5% agarose gel. The relative expression level was deduced from a standard curve constructed using the positive control sample and normalized against the expression level of HPRT in each sample.

Protein Kinase-inhibitory Assay—Serum-deprived HAT-7 cells were plated in 6-well plates and treated with 0.5 μM K-252a (*Trk* tyrosine kinase inhibitor; Calbiochem) and 100 nM TAT-Pep5 (p75NTR signaling inhibitor; Calbiochem) prior to treatment with NT-4 for 30 min. After 48 h, total RNA was extracted, and RT-PCR was performed.

Preparation of Tissue Sections and HE Staining—Mouse heads from P1, P3, and P7 wild-type and NT-4 null mice were fixed with 4% paraformaldehyde in PBS overnight at 4 °C. The tissues were decalcified with 250 mM EDTA/PBS for 3 days, dehydrated in xylene through a graded ethanol series, and then embedded in paraffin. Sections were sliced at 8 μm using a microtome (RM2125RT; Leica). For detailed morphological analysis of the molars, the sections were stained with Harris hematoxylin (Sigma) and Eosine Y (Sigma). The widths of enamel matrix and dentin were measured under a microscope (Bisozero-8000).

RESULTS

Expression of NT-4 and TrkB Receptors in the Tooth Germs and Dental Cell Lines—We first examined the expression of NT-4 and *TrkB* receptors in tooth germs and dental cell lines by RT-PCR. In tooth germs of P3 mice, NT-4 was highly expressed in the dental epithelium and weakly expressed in the dental mesenchyme (Fig. 1*A*). The full-length *TrkB-FL* and truncated *TrkB-T1* and *-T2* were expressed in the dental epithelium. On the other hand, *TrkB-T1*, but not *TrkB-FL* or *TrkB-T2*, was expressed in the mesenchyme. Further, p75 expression levels were low in both the epithelium and mesenchyme (Fig. 1*A*). The expression patterns of NT-4, *TrkB*s, and p75 in dental epithelial cell line HAT-7 and dental mesenchyme cell line mDP were similar to those in the tooth germ tissues, except for a low expression level of *TrkB-FL* in mDP cells and a high expression level of p75 in HAT-7 cells (Fig. 1*B*). These results suggest that NT-4, *TrkB-FL*, *TrkB-T1*, and *TrkB-T2* are expressed in the dental epithelium and may regulate differentiation of the dental epithelium.

Inhibition of Proliferation of HAT-7 Cells by NT-4—We next examined the effect of NT-4 on HAT-7 cell proliferation (Fig. 2). HAT-7 cells were treated with NT-4, and cell proliferation was analyzed by BrdUrd incorporation for 1 h. The number of

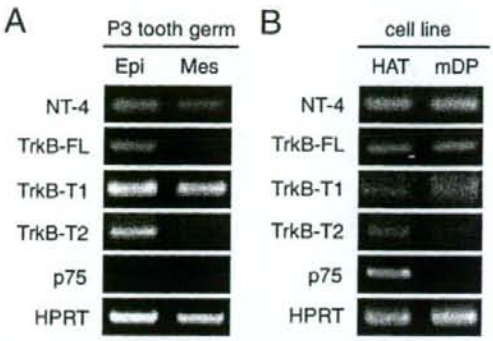

FIGURE 1. **Expression of NT-4 and receptors in tooth germs and dental cell lines.** Tooth germs were dissected from P3 mice, and the dental epithelium (*Epi*) and mesenchyme (*Mes*) were separated under a microscope. Total mRNA from these tissues was amplified using a semiquantitative RT-PCR method with specific primer sets (*A*). Total mRNA expression of NT-4 and *TrkB* receptors in dental epithelial cell line HAT-7 and mesenchymal cell line mDP was analyzed by RT-PCR (*B*).

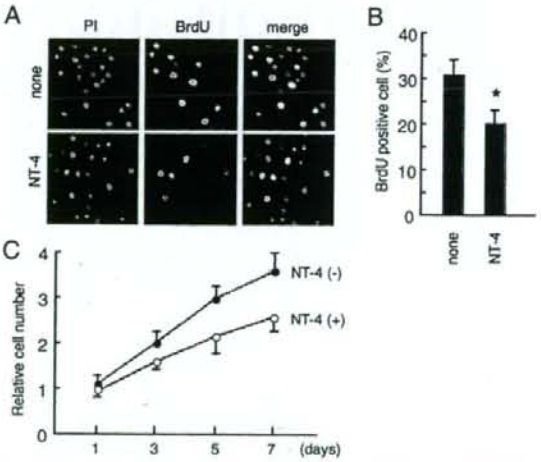

FIGURE 2. **NT-4 inhibits cell proliferation.** Dental epithelial cells (HAT-7) were cultured with NT-4 for 24 h. BrdUrd incorporation after 1 h was analyzed using a fluorescence microscope (*A* and *B*). Cell numbers of HAT-7 cells cultured with or without NT-4 were counted using a trypan blue exclusion method after 1, 3, 5, and 7 days of culture (*C*). These experiments were repeated at least five times with similar results. Statistical analysis was performed using analysis of variance (*, $p < 0.01$).

BrdUrd-positive cells was decreased by 30% after stimulation with NT-4 (Fig. 2, *A* and *B*). We also found that the number of HAT-7 cells was decreased by about 25% when the cells were cultured in the presence of NT-4 for 7 days (Fig. 2*C*). These results indicate that NT-4 inhibits the proliferation of dental epithelial cells in culture.

NT-4 Induces Ambn Expression—To analyze the effects of neurotrophic factors on dental epithelium differentiation, NGF, BDNF, or NT-4 was added to HAT-7 cell cultures. After 48 h, total RNA was analyzed for the expression of ameloblast differentiation markers by RT-PCR. Ambn, Enam, dentin sialophosphoprotein (*Dspp*), osteopontin (*Opn*), and osteonectin (*Osn*) were induced by NGF, BDNF, and NT-4 (Fig. 3, *A* and *B*).

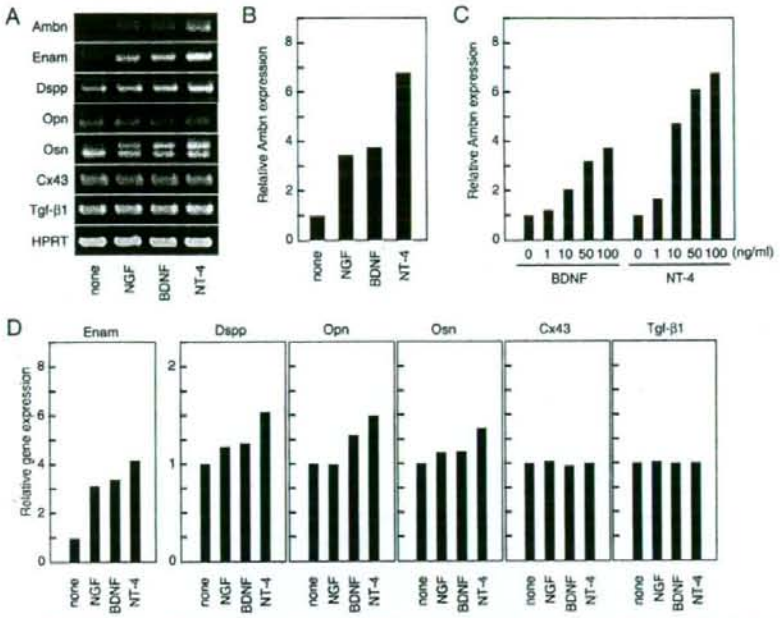

FIGURE 3. **Expression of tooth marker genes in HAT-7 cells with neurotrophic factors.** HAT-7 cells were cultured with 100 ng/ml NGF, BDNF, or NT-4 for 48 h. Total mRNA was analyzed for the expression of various genes by semiquantitative RT-PCR. Ambn, Enam, dentin sialophosphoprotein (*Dspp*), osteopontin (*Opn*), osteonectin (*Osn*), connexin 43 (*Cx43*), and transforming growth factor-β1 (*Tgf-β1*) (*A*). Hprt was used as an internal control. The level of gene expression in the absence of growth factors was set at 1 for comparison (*B* and *D*). HAT-7 cells were stimulated with various amounts of NT-4 and BDNF for 48 h. Hprt expression showed no significant difference between each culture. The level of Ambn expression in cells without factors was set at 1 for comparison (*C*).

Amel was also induced by NT-4 (data not shown). This effect was similar on all of the various amelogenin isoforms. The expression level of Ambn induced by NT-4 was higher than those by NGF or BDNF (Fig. 3*B*). The induction of Ambn expression by BDNF or NT-4 was dose-dependent (Fig. 3*C*), with the higher level by NT-4. The expression of gap junctional proteins (Gja1) and transforming growth factor-β1 was the same between the control and neurotrophic factor-treated cells (Fig. 3*D*). These results indicate that NT-4 induces enamel matrix genes and promotes ameloblast differentiation.

NT-4 and BDNF Induce Expression of Their Receptor but Not p75—Since the expression level of *TrkB* receptors is important for NT-4 signaling, we examined their expression in HAT-7 cells with or without NT-4 by RT-PCR (supplemental Fig. 1). We found that *TrkB-FL*, *TrkB-T1*, and *TrkB-T2* were highly induced by NT-4 and BDNF. NGF also induced the expression of *TrkB-FL* and *TrkB-T1*, but not *TrkB-T2* (supplemental Fig. 1, *A* and *B*).

Overexpression of TrkB-FL Enhances NT-4-mediated Ambn Induction—NT-4 induced expression of Ambn, *TrkB-FL*, and truncated *TrkB*. However, it is not clear which receptor is active for NT-4-mediated Ambn induction. To assess this question, we stably transfected HAT-7 cells with the *TrkB-FL* or *TrkB-T1* expression construct, cultured them with NT-4, and analyzed Ambn expression by RT-PCR. Ambn expression was induced by NT-4 in untransfected cells as shown in Figs. 3, *A* and *B*, and 4*A*. This NT-4-mediated Ambn induction was increased in *TrkB-FL*-transfected cells (Fig. 4, *A* and *B*). The basal level of Ambn expression was also higher in the transfected cells than in untransfected cells. However, in *TrkB-T1*-transfected cells, NT-4-mediated Ambn induction was inhibited (Fig. 4, *A* and *B*). Similar results were obtained from immunohistological analysis using Ambn antibody (data not shown). Furthermore, Ambn expression induced by NT-4 in *TrkB-FL* transfectants was completely inhibited by K252a, a *Trk* tyrosine kinase inhibitor (Fig. 4, *C* and *D*). These results indicate that the induction of Ambn by NT-4 is regulated via *TrkB-FL* but not by truncated *TrkB-T1*.

NT-4 Activates ERK1/2—In neuronal cells, NT-4 induces phosphorylation of *TrkB* and activates the Ras-MEK-ERK1/2 pathway (8). To analyze NT-4 signaling in the dental epithelium, we performed Western blotting using anti-phospho-specific ERK1/2 (MAPK) antibody. Phosphorylation of ERK1/2 was observed at 5 min after stimulation with NT-4 and then disappeared after 30 min (Fig. 5*A*). Further, the level of phosphorylation of ERK2 was higher than that of ERK1 (Fig. 5*B*). Next, we examined the ERK1/2 phosphorylation level in *TrkB*-transfected HAT-7 cells in the presence of NT-4 (Fig. 6, *A* and *B*). *TrkB-FL*-transfected cells showed strong activation of ERK1/2 at 5 min after the NT-4 treatment. However, the activation of ERK1/2 was not observed in *TrkB-T1*-transfected cells. These results indicate that full-length *TrkB-FL* is a major *TrkB* receptor for NT-4 signaling, and truncated *TrkB-T1* acts as a dominant negative factor for dental epithelial cells.

Trk Inhibitor K252a Inhibits Ambn Expression—NT-4 binds to *TrkB* and the low affinity receptor p75 and transduces downstream cellular signaling (8). To identify the signaling pathway involved in Ambn expression, we treated HAT-7 cells with the *Trk* inhibitor K252a or p75 inhibitor TAT-pep5 prior to stimulation with NT-4 (Fig. 7, *A* and *B*). NT-4-medaited induction of Ambn was significantly inhibited by K252a and TAT-pep5. Moreover, the induction of *TrkB* receptors by NT-4 was also inhibited by K252a and TAT-pep5. The inhibitory effect by K252a was higher than that by TAT-pep5. The MEK inhibitor PD98059 inhibited phosphorylation of neurotrophic factor-induced ERK1/2, and PD98059 treatment also inhibited the NT-4-mediated Ambn induction in HAT-7 cells (data not shown). These results suggest that ligand-induced activation of *TrkB* and p75 is important for the expression of Ambn, *TrkB-FL*, and *TrkB-T1*.

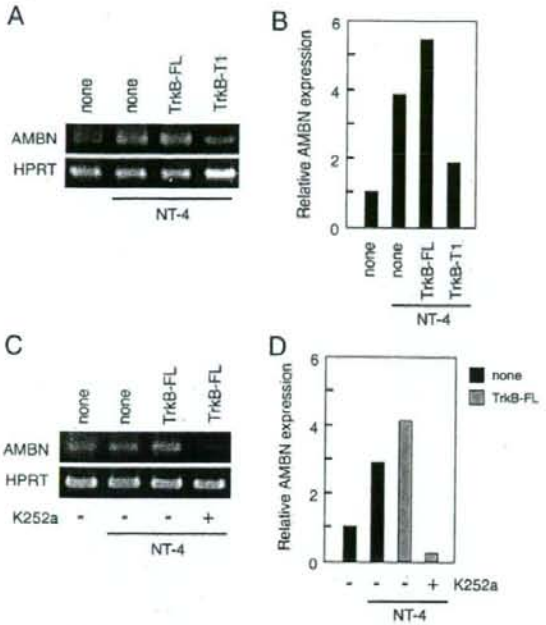

FIGURE 4. **Increase in NT-4-mediated Ambn induction in HAT-7 cells by overexpressing *TrkB-FL*.** The expression constructs for *TrkB-FL* and *TrkB-T1* receptors were stably transfected into HAT-7 cells. The pooled transfected cells were treated with NT-4 for 48 h. Ambn expression was analyzed using RT-PCR (*A*). The level of Ambn expression in the control cells without NT-4 was set at 1 for comparison (*B*). The *TrkB-FL* transfectant cells were cultured with or without K252a in the presence of NT-4 for 48 h and then analyzed for the expression of Ambn (*C*). The level of gene expression in the control cells without NT-4 was set at 1 for comparison (*D*).

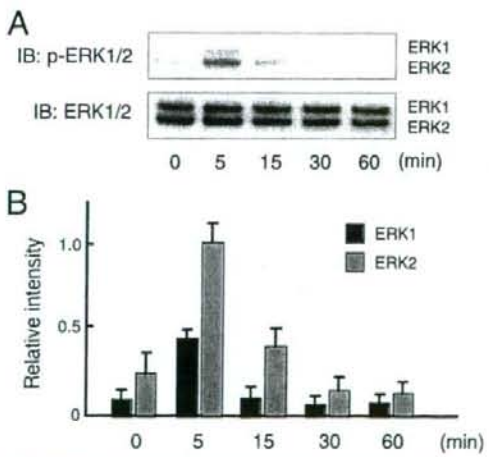

FIGURE 5. **Phosphorylation of ERK1/2 stimulated by NT-4.** The time course of phosphorylation of ERK1/2 after NT-4 treatment was analyzed by Western blotting (*IB*) using the anti-phospho-MAPK antibody (*A*). For the quantitations of *A*, the relative intensity of phosphorylated ERK1/2 (*p-ERK1/2*) in HAT-7 cells after 5 min was set at 1 for comparison (*B*).

NT-4 Null Mice Develop a Thin Enamel Layer and Have Reduced Ambn Expression—We demonstrated that NT-4 promoted epithelia cell differentiation in culture. To examine *in vivo* function of NT-4 in tooth development, we analyzed molars of NT-4 null mice (Fig. 8). NT-4 expression was completely absent in tooth germs of P1, P3, and P7 mice (supplemental Fig. 3). The expression of *TrkB* in NT-4 null tooth germs was similar to that of heterozygotes and wild-type mice (data not shown). We found that P3 molars had a thinner enamel matrix layer than control, whereas there was no significant difference in the predentin and dentin (Fig. 8, *A* and *B*). The size, shape, and polarization of ameloblasts in the mutant molars were normal as compared with those of the heterozygotes. Furthermore, Ambn expression in NT-4 null tooth germs was reduced as compared with that in heterozygotes (Fig. 8, *C* and *D*). These results suggest that NT-4 regulates Ambn expression and enamel layer formation.

DISCUSSION

Our results show that NT-4 regulates dental epithelial cell differentiation and enamel matrix gene expression via *TrkB-FL* but not via truncated *TrkB* forms. NT-4 inhibited cell proliferation and also induced enamel matrix genes, such as Ambn in dental epithelial cells. NT-4-deficient teeth resulted in a thin enamel layer during the initial stage of amelogenesis. Our findings are the first to show that a neurotrophic factor plays an important role in tooth development.

The functional roles of NT-4 and its receptors have been reported mainly in neuronal tissues. Complete ablation of p75 in mice causes defects in both the nervous and vascular systems (23). Those animals displayed sensory and sympathetic defects, thus demonstrating that the p75 receptor is required for proper neuronal development. *TrkB* mutants display severe phenotypes that result in the death of most mutant mice in the first postnatal week because of their inability to feed (24), whereas NT-4 knock-out mice are viable and fertile but have a 50% loss of neurons in the nodose-petrosal and geniculate ganglia (25, 26). BDNF knock-out mice are characterized by selective sensory disorders and have a reduced number of neurons in sensory ganglia; they do not survive longer than 3–4 weeks after birth (27, 28). Although NT-4 and BDNF use *TrkB* as a receptor, phenotypes of *TrkB*, NT-4, and BDNF knock-out mice differ each other. Thus, it is suggested that NT-4 has a different expression pattern and function from that of BDNF. In fact, NT-4, but not BDNF, is expressed in the inner dental epithelium. During tooth germ development, NGF is expressed in the dental mesenchyme but not in the dental epithelium (20). In contrast, BDNF is found in the dental mesenchyme in the human tooth germ but not in that of mice. In the present study, both NGF and BDNF induced expression of the ameloblast markers, Ambn and Enam, and NT-4 receptors, *TrkB-FL* and *TrkB-T1*. NGF and BDNF may be important for mesenchymal and epithelial interactions. NT-4 was expressed mostly in dental epithelia in tooth germs and has been detected in both dental epithelial and mesenchymal cell lines, suggesting that it functions in an autocrine manner in dental epithelium. We found that p75 was expressed in an undifferentiated dental epithelial cell line but was not detectable in the tooth germ. It was

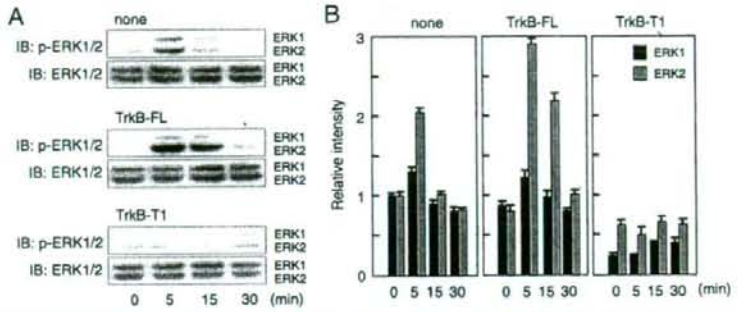

FIGURE 6. **Increase in phosphorylation of ERK1/2 in *TrkB-FL* transfectant cells by NT-4.** The time course of phosphorylation of ERK1/2 in *TrkB-FL*- and *T1*-transfected HAT-7 cells after treatment with NT-4 was analyzed by Western blotting (*IB*) using the anti-phospho-MAPK antibody (*A*). The Western blots with anti-MAPK showed equivalent amounts of total ERK proteins in each *lane*. The relative intensity of p-ERK1 in the control cells at 0 min was set at 1 for comparison (*B*).

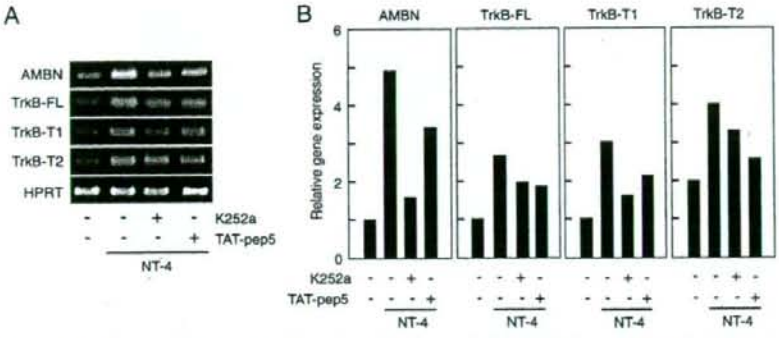

FIGURE 7. **Inhibition of NT-4-mediated induction of Ambn and *TrkBs* by K252a and TAT-pep5.** HAT-7 cells were treated with NT-4 in the presence of K252a or TAT-pep5. The expressions of Ambn, *TrkB-FL*, *TrkB-T1*, and *TrkB-T2* were analyzed by semiquantitative RT-PCR with specific primer sets (*A*). The level of gene expression in the control cells without NT-4 was set at 1 for comparison (*B*).

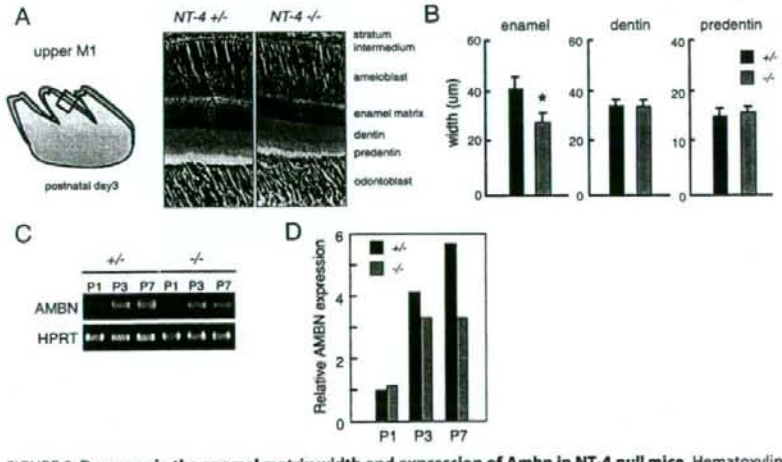

FIGURE 8. **Decrease in the enamel matrix width and expression of Ambn in NT-4 null mice.** Hematoxylin and eosin staining of P3 mouse molars were performed (*A*). The widths of the enamel matrix, dentin, and predentin were measured (*B*). Developing molars from heterozygote and mutant mice were dissected from P1, P3, and P7 mice, and total mRNA was prepared. The expression of Ambn was analyzed by semiquantitative RT-PCR with an Ambn primer set (*C*). The level of Ambn expression in P1 heterozygote mice was set at 1 for comparison (*D*).

reported that in incisors, p75 is expressed in the inner dental epithelium but is completely absent in differentiated ameloblasts (6). Further, the possibility of epithelial-mesenchymal communication within the intact tooth germ, whereas there is complete absence of those effects in the individual cells cultures, may be at the root of the differences of p75 expression between tooth germ and dental epithelial cell cultures. Moreover, p75 expression was not changed after stimulation with neurotrophins, whereas the p75 inhibitor TAT-pep5 was less effective on the expression of Ambn than *Trk* inhibitor K252a. These results suggest that p75 may not be important for the expression of Ambn in ameloblasts.

Truncated *TrkB* receptors have dominant inhibitory effects on BDNF and presynaptic signaling for BDNF-induced synaptic potentiation in cultured hippocampal neurons (29, 30). Truncated *TrkB-T1* mediates neurotrophin-evoked calcium signaling in glia cells (31) and plays a direct signaling role in mediating inositol-1,4,5-trisphoshate-dependent calcium release. In developing teeth, *TrkB-T1*, but not *TrkB-FL* or *TrkB-T2*, is detected by *in situ* hybridization (32). In the present study, all types of *TrkB* were detected in P3 tooth germ epithelia and a dental epithelial cell line. This discrepancy of *TrkB* expression may have occurred because of different detection efficiencies of the methods used. Although both *TrkB-FL* and truncated *TrkB* were induced by NT-4, overexpression of *TrkB-FL* enhanced the expression of Ambn, but *TrkB-T1* had a dominant negative effect on NT-4-induced Ambn expression. In NT-4-null mice, the expression of *TrkB-T1* and *-T2* was not changed from normal levels. These results suggest that truncated *TrkB* does not have an inhibitory effect on Ambn expression induced by NT-4.

Ambn plays an important role in maintaining the differentiation state of ameloblasts, serves as a cell

adhesion molecule, and inhibits the proliferation of the dental epithelium (6). A deficiency of Ambn causes severe enamel hypoplasia, accelerates proliferation of the dental epithelium, and decreases the expression of amelogenin. The Ambn promoter functions in a cell type-specific manner and contains cis-acting elements that function to enhance and suppress transcription (33). The transcription factor Runx2, known as an essential factor for transcription of mineralized tissue genes, is also required for Ambn transcription (33). Site-directed mutagenesis of the Runx2-binding site in the Ambn promoter decreases Ambn promoter activity in the dental epithelium (33). Sp3, a member of the Sp family of transcription factors, is ubiquitously expressed and present in ameloblasts at the presecretory and secretory stages but not the maturation stage. Sp3-deficient embryos show growth retardation and invariably die at birth of respiratory failure (34), and both endochondral and intramembranous ossification are impaired (35). These mice also have a pronounced defect in late tooth formation. In Sp3-null mice, the enamel and dentin layers of teeth are impaired due to the lack of ameloblast-specific gene products, including Ambn. These results indicate that Runx2 and Sp3 are necessary for the expression of Ambn. Our data suggest that NT-4 is also required for a high level of the expression of Ambn. We showed that NT-4 did not have an effect on the expression of Runx2 in the dental epithelium (supplemental Fig. 2). Further, K252a treatment also did not cause any differences in Runx2 or Sp3 expressions. Thus, neurotrophic factor signaling is not required to regulate the expression of Runx2 and Sp3. The ERK-MAPK pathway provides a major link between the cell surface and nucleus to control proliferation and differentiation. The inhibition of MAPK signaling blocks osteoblast-specific gene expression in mature osteoblasts, whereas a constitutive active form of the MAPK intermediate, MEK1, is stimulatory (36). Runx2 is required for cells to respond to MAPK *in vitro* (37). FGF2 induces osteocalcin expression through MAPK activation in osteoblast cell line and bone marrow stromal cells (40). We demonstrated that in the dental epithelium, ERK phosphorylation was induced by NT-4 and necessary for the phosphorylation of Ambn expression. In fact, the MEK inhibitor PD98059 inhibited ERK phosphorylation and Ambn expression in dental epithelium (data not shown). These results suggest that NT-4-*TrkB*-ERK signaling is important for Ambn expression and ameloblast differentiation.

REFERENCES

1. Thesleff, I., Vaahtokari, A., and Partanen, A. M. (1995) *Int. J. Dev. Biol.* **39,** 35–50
2. Zeichner-David, M., Diekwisch, T., Fincham, A., Lau, E., MacDougall, M., Moradian-Oldak, J., Simmer, J., Snead, M., and Slavkin, H. C. (1995) *Int. J. Dev. Biol.* **39,** 69–92
3. Fukumoto, S., and Yamada, Y. (2005) *Connect. Tissue Res.* **46,** 220–226
4. Fukumoto, S., Miner, J. H., Ida, H., Fukumoto, E., Yuasa, K., Miyazaki, H., Hoffman, M. P., and Yamada, Y. (2006) *J. Biol. Chem.* **281,** 5008–5016
5. Smith, C. E. (1998) *Crit. Rev. Oral Biol. Med.* **9,** 128–161
6. Fukumoto, S., Kiba, T., Hall, B., Iehara, N., Nakamura, T., Longenecker, G., Krebsbach, P. H., Nanci, A., Kulkarni, A. B., and Yamada, Y. (2004) *J. Cell Biol.* **167,** 973–983
7. Barbacid, M. (1994) *J. Neurobiol.* **25,** 1386–1403
8. Barbacid, M. (1995) *Curr. Opin. Cell Biol.* **7,** 148–155
9. Klein, R., Conway, D., Parada, L. F., and Barbacid, M. (1990) *Cell* **61,** 647–656
10. Middlemas, D. S., Lindberg, R. A., and Hunter, T. (1991) *Mol. Cell Biol.* **11,** 143–153
11. Tsoulfas, P., Soppet, D., Escandon, E., Tessarollo, L., Mendoza-Ramirez, J. L., Rosenthal, A., Nikolics, K., and Parada, L. F. (1993) *Neuron* **10,** 975–990
12. Valenzuela, D. M., Maisonpierre, P. C., Glass, D. J., Rojas, E., Nunez, L., Kong, Y., Gies, D. R., Stitt, T. N., Ip, N. Y., and Yancopoulos, G. D. (1993) *Neuron* **10,** 963–974
13. Verdi, J. M., Birren, S. J., Ibanez, C. F., Persson, H., Kaplan, D. R., Benedetti, M., Chao, M. V., and Anderson, D. J. (1994) *Neuron* **12,** 733–745
14. Mahadeo, D., Kaplan, L., Chao, M. V., and Hempstead, B. L. (1994) *J. Biol. Chem.* **269,** 6884–6891
15. Di Marco, E., Mathor, M., Bondanza, S., Cutuli, N., Marchisio, P. C., Cancedda, R., and De Luca, M. (1993) *J. Biol. Chem.* **268,** 22838–22846
16. Kalcheim, C., Carmeli, C., and Rosenthal, A. (1992) *Proc. Natl. Acad. Sci. U. S. A.* **89,** 1661–1665
17. Sariola, H., Saarma, M., Sainio, K., Arumae, U., Palgi, J., Vaahtokari, A., Thesleff, I., and Karavanov, A. (1991) *Science* **254,** 571–573
18. Rabizadeh, S., Oh, J., Zhong, L. T., Yang, J., Bitler, C. M., Butcher, L. L., and Bredesen, D. E. (1993) *Science* **261,** 345–348
19. Barrett, G. L., and Bartlett, P. F. (1994) *Proc. Natl. Acad. Sci. U. S. A.* **91,** 6501–6505
20. Luukko, K., Arumae, U., Karavanov, A., Moshnyakov, M., Sainio, K., Sariola, H., Saarma, M., and Thesleff, I. (1997) *Dev. Dyn.* **210,** 117–129
21. Nosrat, C. A., Fried, K., Lindskog, S., and Olson, L. (1997) *Cell Tissue Res.* **290,** 569–580
22. Yuasa, K., Fukumoto, S., Kamasaki, Y., Yamada, A., Fukumoto, E., Kanaoka, K., Saito, K., Harada, H., Arikawa-Hirasawa, E., Miyagoe-Suzuki, Y., Takeda, S., Okamoto, K., Kato, Y., and Fujiwara, T. (2004) *J. Biol. Chem.* **279,** 10286–10292
23. von Schack, D., Casademunt, E., Schweigreiter, R., Meyer, M., Bibel, M., and Dechant, G. (2001) *Nat. Neurosci.* **4,** 977–978
24. Klein, R., Smeyne, R. J., Wurst, W., Long, L. K., Auerbach, B. A., Joyner, A. L., and Barbacid, M. (1993) *Cell* **75,** 113–122
25. Conover, J. C., Erickson, J. T., Katz, D. M., Bianchi, L. M., Poucymirou, W. T., McClain, J., Pan, L., Helgren, M., Ip, N. Y., Boland, P., Friedman, B., Wiegand, S., Vejsada, R., Kato, A. C., Dechiara, T. H., and Yancopoulos, G. D. (1995) *Nature* **375,** 235–238
26. Liu, X., Ernfors, P., Wu, H., and Jaenisch, R. (1995) *Nature* **375,** 238–241
27. Ernfors, P., Lee, K. F., and Jaenisch, R. (1994) *Nature* **368,** 147–150
28. Korte, M., Carroll, P., Wolf, E., Brem, G., Thoenen, H., and Bonhoeffer, T. (1995) *Proc. Natl. Acad. Sci. U. S. A.* **92,** 8856–8860
29. Eide, F. F., Vining, E. R., Eide, B. L., Zang, K., Wang, X. Y., and Reichardt, L. F. (1996) *J. Neurosci.* **16,** 3123–3129
30. Li, Y. X., Xu, Y., Ju, D., Lester, H. A., Davidson, N., and Schuman, E. M. (1998) *Proc. Natl. Acad. Sci. U. S. A.* **95,** 10884–10889
31. Rose, C. R., Blum, R., Pichler, B., Lepier, A., Kafitz, K. W., and Konnerth, A. (2003) *Nature* **426,** 74–78
32. Luukko, K., Moshnyakov, M., Sainio, K., Saarma, M., Sariola, H., and Thesleff, I. (1996) *Dev. Dyn.* **206,** 87–99
33. Dhamija, S., and Krebsbach, P. H. (2001) *J. Biol. Chem.* **276,** 35159–35164
34. Bouwman, P., Gollner, H., Elsasser, H. P., Eckhoff, G., Karis, A., Grosveld, F., Philipsen, S., and Suske, G. (2000) *EMBO J.* **19,** 655–661
35. Gollner, H., Dani, C., Phillips, B., Philipsen, S., and Suske, G. (2001) *Mech. Dev.* **106,** 77–83
36. Xiao, G., Gopalakrishnan, R., Jiang, D., Reith, E., Benson, M. D., and Franceschi, R. T. (2002) *J. Bone Miner. Res.* **17,** 101–110
37. Ducy, P., Zhang, R., Geoffroy, V., Ridall, A. L., and Karsenty, G. (1997) *Cell* **89,** 747–754
38. Xiao, G., Jiang, D., Thomas, P., Benson, M. D., Guan, K., Karsenty, G., and Franceschi, R. T. (2000) *J. Biol. Chem.* **275,** 4453–4459
39. Franceschi, R. T., Xiao, G., Jiang, D., Gopalakrishnan, R., Yang, S., and Reith, E. (2003) *Connect. Tissue Res.* **44,** Suppl. 1, 109–116
40. Xiao, G., Jiang, D., Gopalakrishnan, R., and Franceschi, R. T. (2002) *J. Biol. Chem.* **277,** 36181–36187

Cell Tissue Res (2008) 331:447–459
DOI 10.1007/s00441-007-0532-1

REGULAR ARTICLE

Collagen type I matrix affects molecular and cellular behavior of purified porcine dental follicle cells

S. Tsuchiya · M. J. Honda · Y. Shinohara · M. Saito · M. Ueda

Received: 13 April 2007 / Accepted: 1 October 2007 / Published online: 13 November 2007

Abstract We investigated porcine dental follicle cells at the early crown-formation stage and examined the behavior of cells grown in a collagen type I (Col-I) matrix. Clone-porcine dental follicle cells (DFC-I) and controls, viz., dental follicle itself, nonclone-dental follicle cells, periodontal ligament cells (PDLC), and bone marrow stromal cells, were obtained from 6-month-old pigs. DFC-I showed a different gene expression pattern from controls by reverse-transcription polymerase chain reaction analysis. In addition, Col-I treatment enhanced DFC-I proliferation and increased their alkaline phosphatase activity compared with nontreated DFC-I. The expression of periostin, biglycan, and osteocalcin (OCN) in cells growing on collagen was upregulated, similar to the pattern seen in PDLC. DFC-I with and without Col-I treatment were combined with β-tricalcium phosphate particles and implanted into immunodeficient mice. Significant differences were found in the gene expression patterns of bone sialoprotein, OCN, and periostin in both treated and nontreated implants at 2 and/or 4 weeks. The results showed that Col-I induced the mineralization pathway in these cells. Hard tissue formation was observed in both implant types at 8 weeks. Our results suggest that Col-I facilitates the differentiation of DFC-I along the mineralization process.

Keywords Characterization · Clonal dental follicle cell · Collagen type I matrix · Dental follicle · Mineralization · Porcine

This work was supported in part by grants from the Japanese Ministry of Education, Culture, Sports, Science, and Technology (Kakenhi Kiban B 16390578 and Houga 18659592 to M.J.H.) and by the Hitachi Medical Corporation (Japan) and DENICS International (Japan).

S. Tsuchiya · M. J. Honda (✉) · Y. Shinohara · M. Ueda
Tooth Regeneration, The Division of Stem Cell Engineering,
The Institute of Medical Science, The University of Tokyo,
4-6-1 Shiroganedai, Minato-ku,
Tokyo 108-8639, Japan
e-mail: honda-m@ims.u-tokyo.ac.jp

S. Tsuchiya · M. Ueda
Department of Oral and Maxillofacial Surgery,
Nagoya University Postgraduate School of Medicine,
65 Tsurumacho, Showa-ku, Nagoya,
Aichi 466-8550, Japan

M. Saito
Department of Operative Dentistry and Endodontics,
Kanagawa Dental College,
82 Inaokacho, Yokosuka,
Kanagawa 238-8580, Japan

Introduction

The dental follicle (DF) is a loose, ectomesenchymally derived, connective tissue surrounding the enamel organ and the dental papilla of the developing tooth germ prior to eruption. The differentiation and function of dental follicle cells (DFC) are controlled by a network of regulatory molecules, including growth factors and cytokines (Thesleff and Mikkola 2002). Although the exact sequence of events and cells involved in the development of the periodontium is not established, previous studies have suggested that DFC populations also contain cementoblasts, periodontal ligament cells (PDLC), and osteoblast progenitor or precursor cells (Morsczeck et al. 2005; Palmer and Lumsden 1987; Ten Cate and Mills 1972; Ten Cate et al. 1971; Yoshikawa and Kollar 1981). Bovine DFC isolated from developing tooth germ at the root-forming stage can differentiate into cementoblasts on implantation into immunodeficient mice (Handa et al. 2002). However, the mechanisms regulating DFC differentiation remain poorly understood (Bartold et al. 1988; Diekwisch 2001; Saygin et al. 2000).

In the first part of this study, we isolated porcine DFC from third molars extracted at the early crown-formation stage. Using semiquantitative and real-time reverse-transcription polymerase chain reaction (sq-PCR and rt-PCR), we examined the expression of periodontal- and bone-related genes in these cells and compared them with the gene expressions of PDLC and bone marrow stromal cells (BMSC). The periodontal ligament (PDL) originates from DFC and contains heterogeneous cell populations (Lekic et al. 2001; Murakami et al. 2003). Recent findings suggest that PDLC have many osteoblast-like properties including the expression of bone-associated markers (Han and Amar 2003; Lekic et al. 2001; Marcopoulou et al. 2003; Ouyang et al. 2000; Pitaru et al. 2002). BMSC represent a population of nonhematopoietic marrow-derived cells, and their ability to differentiate into mesenchymal lineage includes osteoprogenitor cells (Bianco et al. 2001; Ducy et al. 1999). Recently, the skeletal site-specific characterization of orofacial BMSC was examined by Akintoye et al. (2006). Clone-porcine DFC (DFC-I) were derived from a single cell and were shown to adhere to a plastic substratum and to be clonogenic and competent to proliferate in vitro.

The extracellular matrix (ECM) relays complex signals from the cell microenvironment to direct proliferation and differentiation during tissue development. However, the role of the ECM and adhesion in DFC differentiation is poorly understood. BMSC undergo osteogenic differentiation in vitro when cultured on a collagen type I (Col-I) matrix (Mizuno and Kuboki 2001; Xiao et al. 1998). Moreover, Col-I also supports osteogenesis in BMSC and may induce differentiation in the absence of soluble osteoinductive factors (Klees et al. 2005; Salasznyk et al. 2004). Col-I is also a major organic component of the predentin-dentin matrix (Ruch 1998), and immature adult rat dental pulp cells strongly induces mRNA expression for dentin sialoprotein in Col-I gel cultures (Nakao et al. 2004). We have therefore hypothesized that Col-I might facilitate the differentiation of DFC. To test this, we cultured DFC on either dishes coated with purified Col-I (Col-I-d) or standard tissue-grade polystyrene dishes (P-d) and analyzed cell growth, alkaline phosphatase (ALPase) activity, and the expression of osteogenic differentiation-related marker genes. The gene expression patterns of Col-I-exposed DFC resembled that of PDLC. Periostin, biglycan, and osteocalcin (OCN) mRNAs were expressed, but bone sialoprotein (BSP) gene expression was absent.

As the final experiment in this study, we examined whether DFC-I could form hard tissue and assessed the effect of Col-I. The differentiated cells showed greater capacity to form hard tissue in vivo than the untreated cells. Our data presented herein provide new insights that Col-I affects the molecular and cellular behavior of purified porcine DFC.

Materials and methods

Isolation of highly purified DFC

As a preliminary experiment, mandibular third molar tooth buds were surgically removed from a 6-month-old porcine jaw and observed by histology and immunohistochemistry to establish the histogenesis (Fig. 1a–c). The DF and enamel organ were dissected as described previously (Wise et al. 1992). Briefly, the isolated DF was placed in 1% trypsin/1 mM EDTA (Invitrogen, Life Technologies, N.Y.) for 10 min at room temperature. The DF was separated from the dental enamel organ by microdissection and then incubated in 0.25% trypsin/1 mM EDTA (Invitrogen) for 10 min at 37°C to dissociate the porcine DFC. Approximately 3.0×10^6 DFC were obtained from one tooth bud. The DFC were cultured in Dulbecco's modified Eagle's medium (DMEM; Kohjin Bio, Saitama, Japan) containing 10% fetal bovine serum (Invitrogen), 2 mM penicillin-streptomycin-glutamine (Invitrogen), and 1 mM sodium pyruvate (Invitrogen) at 37°C in an atmosphere containing 5% CO_2. The medium was changed every 3 days until the third passage. DFC were then suspended at a density of 1 cell per 100 μl and seeded into three 96-well culture plates (Greiner Bio-one, Kremsmuenster, Austria). The cells were incubated for 2 weeks, and then six colonies (each from a single cell) were observed and subsequently subcultured. For the following experiments, the clonal cell populations that had the greatest proliferation rate were subcultured until the tenth passage (DFC-I; Fig. 2a,b). The DFC-I were grown to a maximum of 30 passages.

For comparison, cells were obtained from the PDL attached to the middle portion of the permanent incisor root and the alveolar bone surrounding the first molar tooth. These tissues were digested with 2 mg/ml collagenase (WAKO, Osaka, Japan), and the cells released were maintained as porcine PDLC (Fig. 2c,d) and porcine BMSC (Fig. 2e,f), respectively. The PDLC and BMSC at the third passages were used for following experiments.

Immunofluorescent staining

We tested whether the DFC-I were derived from the DF by using mesenchyme markers. DFC-I grown on coverslips were fixed with 4% paraformaldehyde for 10 min at room temperature and then treated with 0.5% Triton-X 100 (Sigma, St. Louis, Mo.) for 5 min to render them permeable. After the blocking of non-specific sites, the cells were treated for 60 min with sheep antibody to pig Col-I (gift from Dr. J. Sodek, University of Toronto, Canada) diluted 1:20 with phosphate-buffered saline (PBS), with mouse antibody to vimentin (NeoMarkers, Westinghouse, Calif.) diluted 1:1,000, or with an antibody to cytokeratin14 as a control

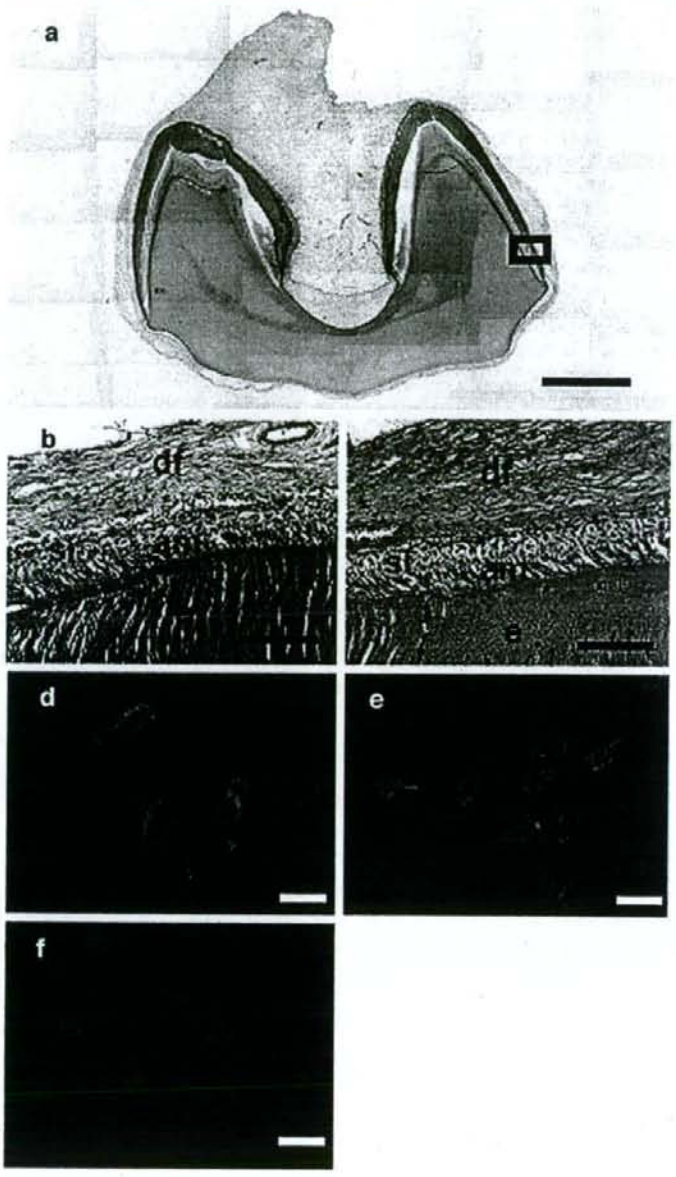

Fig. 1 Morphology of tissue and cells in porcine third molar at the crown-formation stage. **a** Morphology of third molar at the crown-formation stage shown by hematoxylin-eosin staining. Crown formation was well advanced at this stage. **b** Higher magnification of *boxed area* in **a** showing dental follicle (DF; *df*) distinguishable from the dental enamel organ and enamel (*e*). DF fibers were observed running close to the stratum intermedium (*si*) and contained fibroblastic cells (*am* ameloblast); hematoxylin-eosin staining. **c** Strong staining of collagen type I (Col-I) was identified in DF, but not in enamel or in enamel organ. **d**, **e** Immunofluorescence showed strong staining of all clone-porcine dental follicle cells (DFC-I) with specific antibody against vimentin and Col-I, respectively (*blue* DAPI nuclear staining). **f** DFC-I showed no staining with the specific antibody against cytokeratin14. *Bars* 1,000 μm (**a**), 100 μm (**b**, **c**), 10 μm (**d**–**f**)

(1:100 dilution, Chemicon International, Calif.). Rhodamine-conjugated pig anti-rabbit IgG (DakoCytomation, Glostrup, Denmark) and pig anti-sheep IgG (Eappel, Biochemical Division, Auroa, Ohio), both diluted 1:200, were then applied for 60 min at room temperature. The stained cells were mounted and sealed with a PBS-glycerol mixture (1:9 v/v) containing DAPI (4,6-diamidino-2-phenylindole) diluted 1:2,000. Non-immune sera of sheep and rabbit were used instead of primary antibodies as a control.

RNA preparation

Total RNA was isolated, by using TRIZOL REAGENT (Invitrogen Life Technologies) according to the manufac-

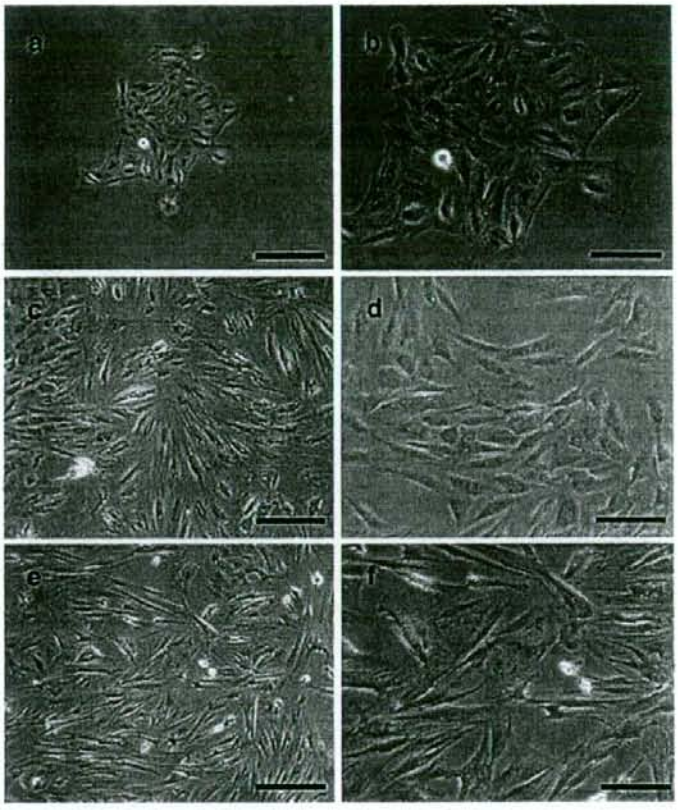

Fig. 2 Cell morphology by phase-contrast microscopy. **a** At culture day 14, DFC-I formed small colonies. **b** Higher magnification of **a** showing the polygonal appearance of the cells at passage 1. **c** At culture day 7, periodontal ligament cells (PDLC) at passage 3 showed a fibroblastic morphology. **d** Higher magnification of **c** showing either spindle- or polygonal-shaped PDLC. **e** At culture day 7, bone marrow stromal cells (BMSC) at passage 3 were more fibroblastic in morphology than the PDLC. **f** At higher magnification, BMSC were either spindle or polygonal in shape. *Bars* 100 μm (**a**, **c**, **e**), 50 μm (**b**, **d**, **f**)

turer's instructions, from the DF at the early crown-formation stage, DFC at the 10th passage, DFC-I at the 10th passage cultured on P-d and Col-I-d, PDLC, BMSC, and implants at 1, 2, and 4 weeks after transplantation.

RNA analyses

cDNA were synthesized from 1 μg total RNA in a 20-μl reaction containing 10× reaction buffer, 5 mM dNTP mixture, 1 U/μl RNase inhibitor, 0.25 U/μl reverse transcriptase (M-MLV reverse transcriptase, Invitrogen), and 0.125 μM random primers (Takara, Tokyo, Japan). For sq-PCR, amplification was performed in a PCR Thermal Cycler SP (Takara) for 25-35 cycles according to the following reaction profile: 95°C for 30 s, 45-60°C for 30 s, and 72°C for 30 s. Porcine glyceraldehyde-3-phosphate dehydrogenase (GAPDH) primers were used as internal standards. The percentage of mRNA expression in the implants from the in vivo gene expression analysis was measured by using Scion Image picture-imaging software (Scion, Frederick, Md.). Synthesized cDNA served as a template for subsequent PCR amplification with specific primers as listed in Table 1.

Real-time PCR was performed to quantify absolute mRNA expression by using the ABI PRISM 7900HT (Applied Biosystems, CA) with Absolute QPCR SYBR Green Mixes (Applied Biosystems). Primers were designed by using Primer-Express software (Applied Biosystems); the sequences are listed in Table 2. The thermocycling parameters were optimized at 50°C for 2 min, 95°C for 15 min, and 40 cycles of 95°C for 15 s and 61°C for 1 min. Cycle threshold (Ct) values were determined and employed to calculate relative gene amounts. The specificity of the PCR products was evaluated from the melt temperature (Tm) of the PCR products by using dissociation curve analysis. PCR products were quantified by means of Microsoft Excel (Microsoft, Wash.) to compare the amplification of the target genes with that of GAPDH as a reference gene, with calibrator normalization and amplification efficiency correction. All experiments were repeated three times, and significant statistical differences were determined by Student's *t*-test ($P<0.05$).